Mon. Not. R. Astron. Soc. **317**, 667–686 (2000)

An Hα survey of eight Abell clusters: the dependence of tidally induced star formation on cluster density

C. Moss[1]★ and M. Whittle[2]

[1]*Vatican Observatory Research Group, Steward Observatory, University of Arizona, Tucson, AZ 85721, USA*
[2]*Department of Astronomy, University of Virginia, Charlottesville, VA 22903, USA*

Accepted 2000 May 1. Received 2000 March 1; in original form 1999 November 30

ABSTRACT

We have undertaken a survey of Hα emission in a substantially complete sample of CGCG galaxies of types Sa and later within 1.5 Abell radii of the centres of eight low-redshift Abell clusters (Abell 262, 347, 400, 426, 569, 779, 1367 and 1656). Some 320 galaxies were surveyed, of which 116 were detected in emission (39 per cent of spirals, 75 per cent of peculiars). Here we present previously unpublished data for 243 galaxies in seven clusters.

Detected emission is classified as 'compact' or 'diffuse'. From an analysis of the full survey sample, we confirm our previous identification of compact and diffuse emission with circumnuclear starburst and disc emission respectively. The circumnuclear emission is associated either with the presence of a bar, or with a disturbed galaxy morphology indicative of ongoing tidal interactions (whether galaxy–galaxy, galaxy–group, or galaxy–cluster).

The frequency of such tidally induced (circumnuclear) starburst emission in spirals increases from regions of lower to higher local galaxy surface density, and from clusters with lower to higher central galaxy space density. The percentages of spirals classed as disturbed and of galaxies classified as peculiar show a similar trend. These results suggest that tidal interactions for spirals are more frequent in regions of higher local density and for clusters with higher central galaxy density. The prevalence of such tidal interactions in clusters is expected from recent theoretical modelling of clusters with a non-static potential undergoing collapse and infall. Furthermore, in accord with this picture, we suggest that peculiar galaxies are predominantly ongoing mergers.

We conclude that tidal interactions are likely to be the main mechanism for the transformation of spirals to S0s in clusters. This mechanism operates more efficiently in higher density environments, as is required by the morphological type–local surface density (T–Σ) relation for galaxies in clusters. For regions of comparable local density, the frequency of tidally induced starburst emission is greater in clusters with higher central galaxy density. This implies that, for a given local density, morphological transformation of disc galaxies proceeds more rapidly in clusters of higher central galaxy density. This effect is considered to be the result of subcluster merging, and could account for the previously considered anomalous absence of a significant T–Σ relation for irregular clusters at intermediate redshift.

Key words: stars: formation – galaxies: clusters: general – galaxies: evolution – galaxies: interactions – galaxies: spiral.

1 INTRODUCTION

The systematic differences in morphology between field and cluster galaxy populations have long been known (e.g. Hubble & Humason 1931; Oemler 1974). More recently, data from the *HST* have shown the remarkable changes in cluster galaxy populations between intermediate redshifts ($z \sim 0.5$) and the present. Intermediate-redshift clusters contain a large population of blue, star-forming galaxies, which have been shown to be predominantly normal spiral and irregular galaxies, a fraction of which are

★ E-mail: cmm@astro.livjm.ac.uk

interacting or obviously disturbed (e.g. Butcher & Oemler 1978; Dressler et al. 1994; Oemler, Dressler & Butcher 1997; Smail et al. 1997). They constitute up to 50 per cent of the cluster population, but by the present epoch have been depleted by a factor of 2 in rich clusters and have been replaced by a corresponding increase in the S0 population (Oemler 1974; Dressler 1980; Dressler et al. 1997). What processes are responsible for this rapid depletion of the spiral population and corresponding increase in S0s in rich clusters since $z = 0.5$? There have been many suggested mechanisms, either to remove gas and/or to induce star formation, some of which depend on galaxy–galaxy collisions (e.g. Spitzer & Baade 1951; Miller 1988; Valluri & Jog 1990), or on the effect of the intracluster medium (e.g. Gunn & Gott 1972; Cowie & Songaila 1977), or on tidal shocks whether from galaxy–galaxy or cluster–galaxy interactions (e.g. Noguchi & Ishibashi 1986; Lavery & Henry 1988; Sanders et al. 1988; Henriksen & Byrd 1996; Moore et al. 1996).

Nearby rich clusters have a residual population of spiral galaxies. If one or several of the proposed mechanisms have been operating to transform spirals into S0s over the relatively short look-back time to $z = 0.5$, it is clear that we might expect the same processes to be continuing to operate in the present on the residual population of spirals in clusters. These processes can be more easily studied in nearby clusters than at higher redshifts. Furthermore, all of the proposed mechanisms involve potentially dramatic changes in the star formation rates in spirals. Thus a comparison of star formation rates between spirals in nearby clusters and those in the field may provide the observational evidence to help decide the physical mechanism which has been responsible for the dramatic recent change in the cluster disc galaxy population.

In practice, it has proved difficult to establish agreement amongst different authors regarding changes of star formation rate between field and cluster spirals. However, much recent work supports either similar or enhanced star formation in cluster spirals compared to field spirals (e.g. Donas et al. 1990; Moss & Whittle 1993, hereafter Paper II; Gavazzi & Contursi 1994; Biviano et al. 1997; Moss, Whittle & Pesce 1998, hereafter Paper III; Gavazzi et al. 1998). Biviano et al. have suggested that earlier studies which claimed reduced star formation in cluster spirals may have been affected by an unrecognized bias whereby faint field galaxies are more likely to be detected in emission than their cluster counterparts. Two recent studies (Balogh et al. 1998; Hashimoto et al. 1998) have found a suppression of star formation in cluster galaxies relative to galaxies of similar morphological type in the field. However, the morphological classifications in these studies are based on bulge-to-disc ratio, and it is not clear to what extent the results are affected by the variation of S0/S ratio from the field to the cluster (see Section 4.1.1 below for further discussion). Furthermore, it is also increasingly evident that star formation in the spiral discs and in the circumnuclear region may have very different dependencies on environment (cf. Paper III; Hashimoto et al. 1998).

We have made an extensive survey of Hα emission as an indicator of the star formation rate in spirals in nearby clusters (Paper III, and references therein). One motivation is to understand how the cluster environment affects the evolution of spiral galaxies, including the dramatic depletion of cluster spirals over the past few giga-years. Our survey technique can distinguish well between disc emission and circumnuclear starburst emission, and accordingly we can investigate how these vary with environment. In previous work we have discussed in detail a comparison between emission in field spirals and a single cluster, Abell 1367 (Paper III). Here we utilize data for all eight clusters in our sample, and do a comparable analysis for a full range of cluster types, discussing how emission varies across a range of environments of differing galaxy densities. We also attempt to differentiate the dependence of emission on local galaxy density from that on cluster type, to give further insight into evolutionary mechanisms operating on cluster spirals.

The paper is set out as follows. In Section 2 we describe the survey sample and summarize observational and emission detection methods. A previously unpublished list of emission-line galaxies (ELGs) detected for six of the eight surveyed clusters is given in Section 3. In this section we also consider the relation of emission to galaxy properties, and show that compact and diffuse emission detected on the prism plates can be well understood as circumnuclear starburst and normal disc emission respectively. In Section 4, using a variety of cluster/field parameters, we show that there is a systematic enhancement of tidally induced starburst emission with increasingly rich clusters. For the richest clusters this enhancement is greater than would be expected simply on the basis of increasing galaxy density alone. These observational results are discussed in Section 5, where we show that they provide convincing evidence that spirals have been transformed to S0s in clusters predominantly by tidal forces, a picture fully in accord with the most recent numerical simulations of clusters (e.g. Gnedin 1999). We further discuss how the observational results can explain the apparently anomalous result for type–galaxy surface density relation found by Dressler et al. (1997) for low-richness clusters at intermediate redshifts. A summary of our results is given in Section 6.

2 OBSERVATIONS AND MEASUREMENTS

2.1 Cluster and galaxy samples

Table 1 gives basic data for the eight Abell clusters in our survey (Abell 262, 347, 400, 426, 569, 779, 1367 and 1656). These clusters constitute a representative sample, comprising all but two of the 10 Abell clusters in the northern hemisphere with redshifts less than $7200\,\mathrm{km\,s^{-1}}$ (the other two clusters, Abell 189 and 194, are both relatively poor clusters comparable to Abell 262, 347, 569 and 779).

Our initial sample of galaxies comprised all CGCG galaxies (Zwicky et al. 1960–1968) within 1.5 Abell radii of the cluster centres (759 galaxies, where resolved double galaxies are counted as two). These galaxies were morphologically classified (see Section 2.3.2) and a subset defined which excluded galaxies with Hubble types E, E/S0, S0 and S0/a, or galaxies of indeterminate type (292 galaxies remaining). A further 28 spirals falling beyond 1.5 Abell radii were included (27 in Abell 1367, one in Abell 400), yielding a final total of 320 galaxies selected for the survey for Hα emission. Our restriction to CGCG galaxies reflects the fact that our detection efficiency decreases sharply below the CGCG magnitude limit $m_{\mathrm{p}} = 15.7$, and our exclusion of E, E/S0, S0 and S0/a galaxies reflects the fact that in practice these Hubble types are rarely detected in Hα (see Paper III). In the case of double galaxies, those 11 individual members fainter than 15.7 were excluded from the statistical sample, as were 15 galaxies which, for various reasons, were visible on only one of our two plates. Thus our final statistical sample represents a substantially complete group of potentially detectable star-forming galaxies in and around nearby Abell clusters.

Table 1. Clusters included in the Hα survey.

Cluster	Cluster centre R.A. (1950)		Dec.		l	b	Abell radius (arcmin)	z_o	σ_v (km s^{-1})	n
Abell 262	1^h	49^m.9	35°	54′	136°.59	−25°.09	105	0.0163	494	47
Abell 347	2	22.7	41	39	141.17	−17.63	91	0.0189	582	21
Abell 400	2	55.0	5	50	170.25	−44.93	72	0.0238	610	71
Abell 426	3	15.3	41	20	150.39	−13.38	96	0.0179	1277	114
Abell 569	7	5.4	48	42	168.58	22.81	88	0.0196	444	12
Abell 779	9	16.8	33	59	191.07	44.41	75	0.0230	472	24
Abell 1367	11	41.9	20	7	234.81	73.03	80	0.0214	822	93
Abell 1656	12	57.4	28	15	58.09	87.96	74	0.0232	880	226

Cluster centres are taken from Abell, Corwin & Olowin (1989). Cluster mean redshifts, z_o, and velocity dispersions, σ_v, based on a total of n redshifts, are taken from Struble & Rood (1991), where z_o has been corrected to the centroid of the Local Group following RC2 (de Vaucouleurs, de Vaucouleurs & Corwin 1976). The Abell radius is defined (Abell 1958) as $5.13 \times 10^5 / cz_o$ arcmin, and corresponds to $\sim 1.5h^{-1}$ Mpc, where h is the Hubble constant in units of 100 km s^{-1} Mpc^{-1}.

Table 2. Plate material.

Plate no.	U.T. date	Cluster	Plate centre R.A. (1950)		Dec.		Prism	Filter	Exp. (min)	Tel. (E/W)
15204	1984 Nov 4	Abell 262	1^h	50^m.0	35°	44′	2 + 4	RG 645	60	E
15205	1984 Nov 4	Abell 262	1	50.2	36	13	2 + 4	RG 645	60	W
13046	1981 Dec 16	Abell 347	2	21.9	41	20	10	RG 630	120	W
14559	1983 Oct 29	Abell 347	2	24.7	41	36	10	RG 645	120	E
15198	1984 Nov 2	Abell 400	2	55.5	6	23	2 + 4	RG 645	120	W
15201	1984 Nov 3	Abell 400	2	56.4	5	32	2 + 4	RG 645	90	E
15191	1984 Oct 31	Abell 426	3	16.8	41	30	2 + 4	RG 645	120	W
15195	1984 Nov 1	Abell 426	3	15.7	41	26	2 + 4	RG 645	120	E
15196	1984 Nov 1	Abell 569	7	4.9	48	28	2 + 4	RG 645	120	E
15230	1984 Dec 31	Abell 569	7	5.9	48	57	2 + 4	RG 645	97	W
14078	1983 Apr 4	Abell 779	9	17.3	33	56	10	RG 630	70	E
14193	1983 May 1	Abell 779	9	16.2	33	47	10	RG 630	120	W
14077	1983 Apr 3	Abell 1367	11	37.9	19	59	10	RG 630	75	E
14200	1983 May 3	Abell 1367	11	41.9	20	00	10	RG 630	120	W
15270	1985 Apr 11	Abell 1656	12	58.4	27	58	2 + 4	RG 645	120	E
15271	1985 Apr 11	Abell 1656	12	57.4	28	21	2 + 4	RG 645	120	W

2.2 Plate material and Hα detection

Table 2 gives basic information about the objective-prism plates used for the survey, while Fig. 1 shows the distribution of CGCG galaxies within the Abell clusters, as well as the objective-prism plate boundaries (see Paper III for Abell 1367).

Our survey technique and methods have been described in detail in Paper I (Moss, Whittle & Irwin 1988), and to a lesser extent in Papers II and III. Here we briefly review the methods. All plates were taken on the 61/94-cm Burrell Schmidt telescope at Kitt Peak in conditions of good seeing and transparency, and are consequently of good quality. The plates cover approximately 5° at 94 arcsec mm^{-1} and use an emulsion/filter combination of either IIIaF/RG630(round) or IIIaF/RG645(square), giving ∼350 Å bandpass centred on 6655 Å with a peak sensitivity ∼6717 Å. Two prisms were used, either a high-dispersion 10° prism giving ∼400 Å mm^{-1}, or, when this became unavailable, a lower dispersion 2° + 4° prism combination giving ∼780 Å mm^{-1}. In Paper III we compared the Hα detection efficiency of these two prism combinations, and concluded that they were substantially equivalent. Each cluster was observed twice, with the telescope east and west of the pier to reverse the dispersion direction. Having two such plates not only ensures a more reliable detection of Hα, but also, from the difference in location of the emission, yields relatively accurate measurements of redshift.

Using a low-power binocular microscope (∼12×), the galaxy spectra were inspected for signs of Hα emission, which appears as an Hα image superposed on the dispersed continuum spectrum. In Paper III we analysed the Hα sensitivity limit, and found that the objective-prism technique is 90 per cent complete down to an equivalent width limit of 20 Å for the Hα + [N II] blend, and ∼29 per cent efficient below this limit.

Table 4 gives the surveyed galaxies and Hα detections for seven clusters, while Paper III give these for the eighth, Abell 1367.

2.3 Parameters and ranking

Our statistical analysis requires a range of parameters to characterize galaxy morphology, Hα emission, local environment, and more global environment. We list these parameters in Table 3, together with their quantification as ranked and/or binned data suitable for the non-parametric statistical tests used below (Sections 3.1 and following), and the sample number, n, for each rank or bin. A more detailed description of individual parameters is as follows.

2.3.1 Hα emission

For each detected galaxy, the Hα emission was graded for visibility on a five-point scale (S – strong; MS – medium-strong; M – medium; MW – medium-weak; and W – weak). Similarly, the appearance of the Hα image was classified on a five-point

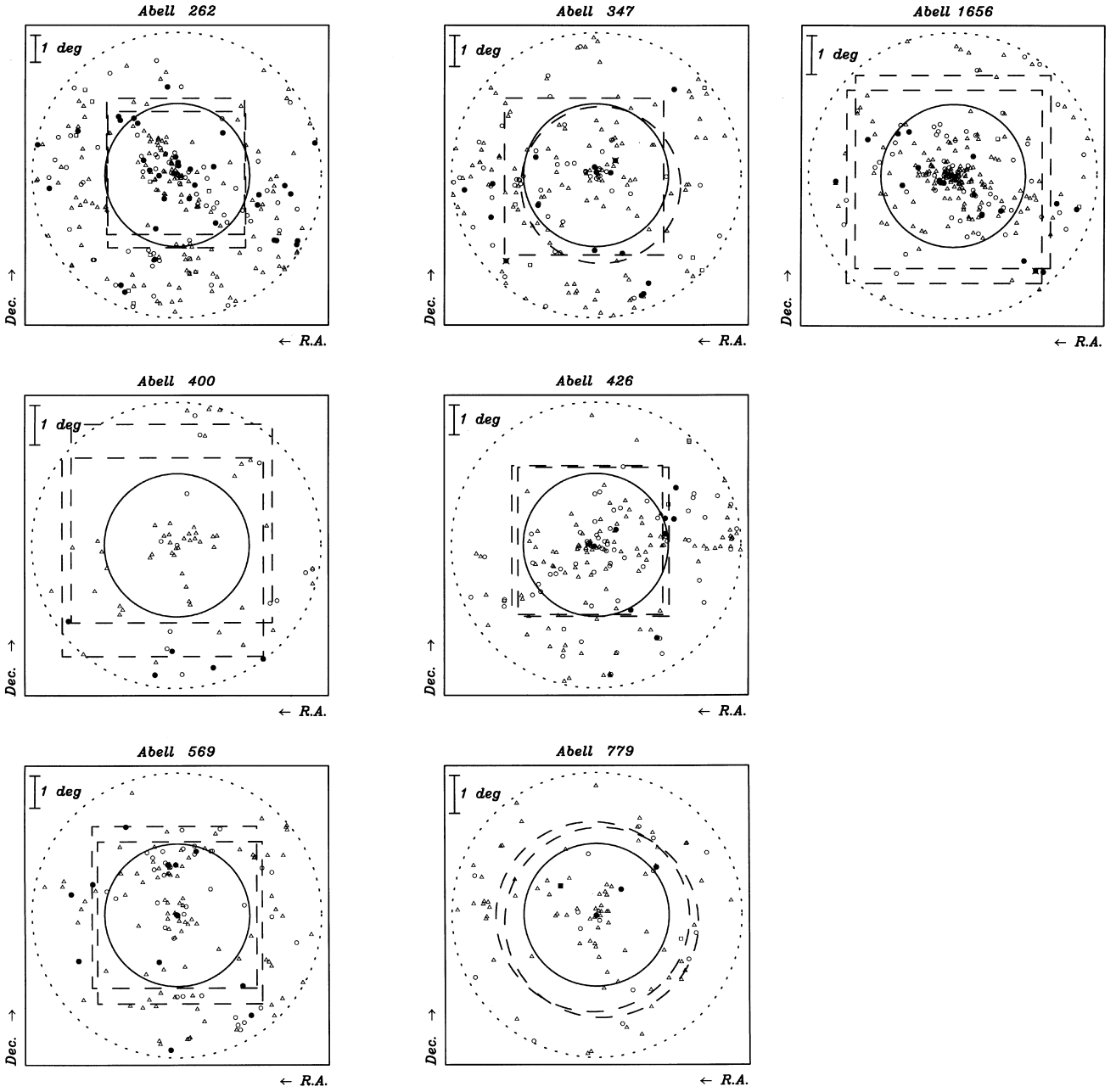

Figure 1. CGCG galaxies in cluster fields. Galaxy symbols are the same as Zwicky et al. (1960–1968): cross superimposed on a filled square, $m_p \leq 11.0$; filled square, $m_p = 11.1$–12.0; open square, $m_p = 12.1$–13.0; filled circle, $m_p = 13.1$–14.0; open circle, $m_p = 14.1$–15.0; open triangle, $m_p = 15.1$–15.7. Plate boundaries are shown schematically with dashed lines. The solid and dotted lines are circles of radius $r = 1.5\ r_A$ and $3.0\ r_A$ respectively, centred on the cluster centre. Note that CGCG galaxies are shown only for $r \leq 3.0\ r_A$.

scale (VC – very concentrated; C – concentrated; N – normal; D – diffuse; and VD – very diffuse). Concentrated emission is much brighter than the underlying continuum and is sharply delineated from it; diffuse emission is only slightly brighter than the continuum and has an indistinct appearance, and in general spans a larger region than the concentrated emission (for further discussion, see Paper II). Galaxies with double, multiple, or offset emission were categorized as compact emission, principally because of its high surface brightness. The combined mean emission classifications from each plate pair are listed in columns 12 and 13 of Table 4.

We choose a binary rank for Hα detection, with no rank assigned for galaxies not satisfactorily surveyed for emission ('?' in Table 4). We also choose binary ranks for the Hα appearance, yielding two parameters: *compact* emission (concentration classes VC, C, or N); and *diffuse* emission (concentration classes D or VD). Astrophysically, we associate compact emission with a circumnuclear starburst, and diffuse emission with more normal ongoing disc-wide star formation. (For further discussion, see Section 3.7 below.)

2.3.2 *Hubble types*

Because star formation rates depend quite sensitively on Hubble type, it is important to estimate these types accurately, so that dependence on environment can be clearly distinguished from

Table 3. Parameters used in the study.

Categories	Rank/[Bin no.]	*n*
Emission		
…	1	180
S,(S),MS,M,MW,W,(W)	2	115
Compact Emission		
…,D,VD	1	236
VC,C,N,DBL	2	58
Diffuse Emission		
…,VC,C,N,DBL	1	238
D,VD	2	56
Type		
Sa	1,[1]	62
Sab	2,[2]	30
Sb	3,[3]	49
Sbc	4,[4]	17
Sc	5,[5]	36
Sc–Irr,Irr	6,[6]	18
S	[7]	21
Peculiar	[8]	62
Bar		
A,A:	1	37
AB,AB:	2	18
B:	3	21
B	4	52
Disturbed		
…	1	210
D::	2	30
D:	3	34
D	4	18
Companion		
…,[C::],[C:],[C]	1	203
C::	2	2
C:	3	18
C	4	25

dependence on Hubble type. Unfortunately, at redshifts of $\sim$6000 km s^{-1} the cluster galaxies are quite small and difficult to type accurately without good plate material. In the case of Abell 1367 we indeed have excellent plate material, and so we used it to perform the typing of most of the CGCG galaxies in that cluster (see Paper III). For the other clusters this is not the case, and we have adopted a somewhat more conservative approach to galaxy typing. For all UGC (Nilson 1973) galaxies, we adopt the UGC type. For non-UGC galaxies, one of us (MW) classified the galaxies on the revised de Vaucouleurs (1959, 1974) system using glass copies of the PSS and direct IIIaJ plates taken on the Burrell Schmidt. The reliability of these types was assessed in two ways. First, UGC galaxies were also typed, and comparison with UGC types showed a standard deviation in the class T of $\sim$1.0. Secondly, all galaxies were independently typed twice and showed similar level of agreement.

For 92 galaxies, it was not possible to determine a reliable type due their small and/or saturated images on the PSS. In Abell 1367 and 1656, some 41 such galaxies with $m_p \leq 15.7$ were inspected for emission on the prism plate pairs for these clusters. A total of six galaxies (15 per cent of the sample) were found to have emission. This is a larger percentage emission detection than for early-type galaxies ($\sim$5 per cent), but much smaller than for galaxies of types Sa and later ($\sim$40 per cent). We conclude that the galaxies with indeterminate type are likely to be predominantly early-type galaxies, and accordingly it was decided also to omit them from the study, as mentioned in Section 2.1. These galaxies should not be confused with 'peculiar' galaxies, nor with spirals with postfix 'pec', both of which have been retained in the sample.

The Hubble types were reduced to eight-category binned data as shown in Table 3, and the spiral stage has been given a simple rank of 1–6. The rank assigned is independent of bar designation or whether 'pec' is appended to the class, but no rank is assigned if a spiral has no stage assigned or the galaxy is classed simply as 'Peculiar'.

2.3.3 *Barred structure*

Since galaxy bars may be related to star formation and environment, we attempted to assign bar designations for all galaxies, following the de Vaucouleurs system. Unfortunately, many UGC types do not distinguish between a non-barred spiral (e.g., SAa) and a spiral with no bar designation (e.g., Sa). Accordingly, we inspected all galaxies for signs of a bar and, where possible, assigned a bar type (e.g., SA, SAB, or SB). This bar classification was included in the type descriptions of the galaxies in the sample given in column 7 of Table 4.

The bar classifications form a rank sequence (1–4; see Table 3) from unbarred (A, A:), through intermediate (AB, AB:), to uncertain bar (B:) and definitely barred (B). Galaxies for which no bar designation can be made are not assigned a rank.

2.3.4 *Disturbance*

We have attempted to classify galaxies on the basis of whether they appear disturbed or not (Table 4, column 8). Clearly, this is important as a possible link to star formation and environment. We adopted a 1–4 rank system, which corresponds to the degree of disturbance (… [no disturbance], D::, D:, D). In assigning disturbance class, information was combined from UGC descriptions and our inspection of direct plate material. Rather uncertain signs of galaxy disturbance (e.g., slight distortion of outer arms, somewhat asymmetric appearance) are assigned D:: (rank 2); more definite signs of distortion (e.g., slight warps, probable tidal plumes, some disturbance) are assigned D: (rank 3); while significantly disturbed galaxies (e.g., bad distortions, strong tidal features, ongoing merger) are classed as D (rank 4). No rank is given to the few galaxies for which it is not possible to decide whether a disturbance is present or not. An effort was made to keep the disturbance classification independent of whether there was a nearby companion or not – it represented a purely morphological rather than environmental classification. Of course, there is considerable overlap between noting a spiral as 'peculiar' and as 'disturbed', although the 'peculiar' note probably refers to a wider variety of anomalous morphologies than just disturbance.

2.3.5 *Nearby companion*

Finally, while inspecting the galaxies a note was made if there was a nearby companion (Table 4, column 9). Although general limits of $>$20 per cent of the size of the galaxy and within $\sim$5 galaxy diameters were applied, the 'companion' assignment was made on a 1–4 rank scale (… [no companion], C::, C:, C) depending on the degree of certainty and/or strength of the interaction. Smaller galaxies further away with no signs of distortion are more likely to be projected companions (C::, rank 2), while larger galaxies closer

Table 4. CGCG galaxies surveyed for Hα emission.

CGCG	UGC	R.A. (1950)	Dec.	r (r_A)	m_p	Type	Dis.	Cp.	$v_\odot$ (km s^{-1})	Ref.	Hα emission Vis.	Conc.	Notes
Abell 262													
521-070	1193	1^h 39^m.5	+35° 23′	1.24	14.1	Sab	…	…	5114	1	…	…	
521-071		1 40.4	+36 20	1.12	15.3	SAB:	…	…	14723	2	…	…	
521-072	1212	1 41.2	+34 9	1.43	14.5	SAb	…	…	10693	1	…	…	
521-073	1220	1 41.6	+37 26	1.29	13.6	S pec	D::	…	5662	1	S	D	
521-074		1 41.7	+34 25	1.28	15.0	S: pec	…	…	5275	2	S	VC	
521-076	1221	1 41.7	+37 57	1.50	15.0	Sbc	…	…	11095	2	…	…	
521-078	1234	1 42.9	+34 52	1.01	14.8	Sc/SBc	D:	…	5653	1	…	…	
521-080	1238	1 43.4	+36 12	0.77	13.5	SA:b	…	…	4515	1	…	…	
521-081		1 43.5	+34 41	1.02	14.7	S: pec	D:	…	5417	1	…	…	
522-003		1 44.0	+34 32	1.04	15.2	pec	D::	…	4205	2	MS	N	
522-004	1248	1 44.3	+35 18	0.74	12.9	Sab	…	…	4756	1	…	…	
522-005	1251	1 44.6	+35 47	0.62	15.0	pec	D	C	4845	2	…	…	
522-006		1 44.8	+34 46	0.88	15.0	SAbc: pec	…	…	5557	1	…	…	
522-007	1257	1 45.2	+36 12	0.57	15.0	SA:ab	…	…	4662	1	…	…	
522-013		1 46.5	+34 44	0.78	15.5	S: pec	D::	C:	4025	1	…	…	
503-030		1 47.7	+33 23	1.46	15.3	S pec	D	…	15086	2	?	?	
522-018	1299	1 47.7	+35 7	0.52	15.7	Irr	…	…	5498	2	…	…	
522-020	1302	1 47.8	+35 2	0.55	13.3	SBb	…	(C::)	4047	1	MS	C	
522-021	1307	1 47.9	+35 40	0.27	15.1	S	…	…	4889	1	MW	C	
522-024	1319	1 48.5	+35 49	0.17	14.5	SA: pec	D::	(C:)	5375	1	W	VD	
522-025		1 49.1	+35 53	0.09	15.6	SAbc:	…	…	6050	1	…	…	
522-029A		1 49.3	+34 55	0.57	(16.4)	S	D:	C			…	…	*
522-029B		1 49.3	+34 55	0.57	(16.4)	S	…	C			…	…	*
522-031	1338	1 49.4	+35 33	0.21	15.2	SAb	…	(C::)	4099	1	…	…	
522-035	1344	1 49.7	+36 15	0.20	14.0	SBa	…	(C::)	3998	1	?	?	
522-038	1347	1 49.8	+36 22	0.27	13.9	Sc/SBc	…	[C:]	4099	1	…	…	
522-041	1349	1 50.0	+35 48	0.06	14.3	SABc	D::	…	6131	1	W	VD	
522-042	1350	1 50.0	+36 15	0.20	14.5	SBb	…	(C::)	5244	1	…	…	
503-044		1 50.1	+33 21	1.46	15.7	S	…	…	11165	2	?	?	
522-050	1361	1 50.9	+36 20	0.27	15.7	Sc	…	C:	5244	1	?	?	
522-051		1 50.9	+36 32	0.38	15.1	SA	…		4686	2	…	…	
522-055	1366	1 51.4	+36 22	0.32	14.7	SBc	…	…	5118	1	…	…	
522-058	1385	1 52.0	+36 41	0.51	14.2	SBa	…	C:	5529	1	S	N	
522-059	1380	1 52.0	+37 5	0.72	15.6	S	…	…	4600	1	…	…	
522-060		1 52.1	+35 11	0.48	15.1	SBab:	…	…	16200	1	…	…	
522-062		1 52.1	+36 41	0.51	15.2	SBb	…	(C:)	5400	1	…	…	
522-063	1387	1 52.2	+36 1	0.27	15.4	S-Irr	D:	(C:)	4502	1	…	…	
522-066	1390	1 52.4	+36 3	0.30	15.5	S	…	…	4368	2	…	…	
522-067		1 52.7	+37 9	0.78	15.5	Sab: pec:	D::	…	14741	2	…	…	
522-069	1398	1 53.0	+36 53	0.67	14.9	SAc:	…	…	5389	1	…	…	
522-071	1400	1 53.2	+35 53	0.38	13.8	Sb	…	C:	4670	1	?	?	
522-073	1404	1 53.4	+36 59	0.74	15.6	SBb	…	…	4458	1	…	…	
522-074	1405	1 53.4	+37 12	0.84	15.7	Sc	…	…	4920	1	…	…	
522-075		1 53.4	+37 15	0.87	15.7	Irr:	…	…	5405	1	…	…	
522-077		1 53.6	+37 5	0.80	15.5	SBb: pec	D::	…	5511	2	M	N	
522-078	1411	1 53.7	+33 56	1.21	13.9	Sb	D::	C:	4748	1	…	…	
522-079		1 53.7	+35 21	0.54	15.3	SA:c:	…	…	5230	2	…	…	
522-081	1416	1 53.8	+36 39	0.62	14.9	S	…	…	5484	1	M	D	
522-082		1 53.9	+35 45	0.47	15.3	SA:c::	…	…	4818	1	?	?	
522-086	1437	1 54.8	+35 40	0.58	12.6	SAB:c	D::	(C:)	4896	1	(S)	D	*
522-088	1441	1 54.9	+37 7	0.90	15.5	Sb	…	…	4996	1	…	…	
522-090		1 55.1	+34 3	1.22	15.7	S: pec	?	…	14279	1	…	…	
522-094	1456	1 56.0	+36 26	0.77	14.0	Sab	…	…	5057	1	…	…	
522-095		1 56.0	+37 30	1.15	15.6	SAB:b:	…	…	14346	1	…	…	
522-096	1459	1 56.1	+35 49	0.72	15.4	Sc	…	…	5466	1	…	…	
522-097	1460	1 56.1	+36 1	0.72	15.0	Sa pec	D::	…	4874	1	…	…	
522-100	1474	1 57.2	+37 21	1.18	15.0	SB(s)dm	…	…	4235	1	MW	VD	
522-102	1493	1 57.9	+37 58	1.49	14.0	SB:ab	…	…	4249	1	W	D	
Abell 347													
538-034		2 10.9	+41 39	1.45	15.0	S	D:	…	4328	1	?	?	
538-037	1738	2 12.8	+42 35	1.36	15.6	Sc	…	[C:]	5734	1	MW	VD	
538-038	1743	2 13.1	+42 35	1.33	15.7	SBb	…	[C:]	13708	1	…	…	
538-040	1780	2 15.9	+40 20	1.21	15.6	Irr	D::	…	5204	1	…	…	
538-043		2 16.9	+41 3	0.82	15.0	pec	D:	…	5936	3	S	DBL	*
538-045	1796	2 17.3	+40 34	0.98	15.5	SAB(s)dm	…	(C:)	6983	1	…	…	
538-046		2 17.4	+41 20	0.69	15.3	SA:b:	…	…	5920	3	W	VD	
538-047		2 18.0	+41 35	0.58	15.6	SB	…	…			…	…	
538-048		2 18.2	+42 39	0.86	15.3	S pec	D:	C:	6639	1	MS	D	
538-050		2 19.1	+42 35	0.76	15.7	Sa:	?	…			…	…	

Table 4 – *continued*

CGCG	UGC	R.A. (1950)		Dec.		r (r_A)	m_p	Type	Dis.	Cp.	$v_\odot$ (km s^{-1})	Ref.	Hα emission Vis.	Conc.	Notes
538-051	1827	2^h	19^m.1	+43°	19′	1.18	15.7	S-Irr	…	…	5810	2	…	…	
538-052	1831	2	19.4	+42	7	0.51	10.8	Sb	…	…	527	1	…	…	
538-053	1832	2	19.4	+42	50	0.88	15.4	Sa	…	…	5913	1	…	…	
538-054		2	19.7	+41	56	0.41	15.7	Sa:	…	(C::)	6390	3	M	VD	
538-056	1840	2	20.0	+41	9	0.47	14.1	pec:	D	C	5425	2	…	…	*
538-058	1842	2	20.2	+41	44	0.31	13.8	Sa	…	(C::)	5400	1	…	…	
538-059		2	20.8	+41	59	0.32	15.7	SBb pec	D:	(C:)			…	…	
538-061	1855	2	21.4	+40	39	0.68	15.1	SBa	…	…	12849	1	…	…	
538-062	1858	2	21.6	+41	28	0.18	15.7	SB	…	…	5304	1	?	?	
538-063		2	21.6	+41	48	0.17	15.7	Sbc	…	…	5680	3	M	VD	
538-066	1866	2	22.0	+41	38	0.09	14.9	SBa	…	(C)	739	1	…	…	
539-014	1868	2	22.1	+41	52	0.16	14.4	SBa	…	(C:)	4586	1	…	…	
539-015		2	22.2	+41	30	0.12	15.7	S	…	(C::)			…	…	
539-023	1887	2	22.9	+41	55	0.18	13.9	SAc	…	(C::)	5548	1	…	…	
539-024		2	23.6	+41	37	0.11	15.0	SBb	…	…	5723	3	S	N	
539-025		2	23.7	+41	28	0.17	15.3	SB pec	D:	(C:)	4316	3	S	N	
539-026		2	23.7	+41	48	0.16	15.7	Sa:	…	(C:)	5548	1	…	…	
539-027		2	23.8	+42	35	0.63	15.7	SB:bc:	…	…			…	…	
539-029		2	24.3	+41	42	0.20	15.7	S	D:	(C:)	6740	3	MS	VD	
539-030	1915	2	24.4	+41	45	0.22	14.4	Sb:	D::	(C)	5638	3	S	D	
539-032	1961	2	26.3	+42	2	0.51	15.0	SB:c	…	…	5631	1	…	…	
539-036	1988	2	28.1	+40	10	1.19	14.7	Sab	…	…	5814	1	S	D	
539-038		2	28.3	+40	2	1.27	15.7	S pec	D::	C	5889	3	S	N	
539-040	1997	2	29.0	+43	14	1.29	15.4	Sb	…	…	6162	1	…	…	
539-041	2001	2	29.2	+41	59	0.83	14.6	Sab	…	(C::)	6989	1	…	…	
539-046	2034	2	30.6	+40	19	1.32	15.0	Irr	…	[C::]	579	2	…	…	
539-048		2	30.8	+42	28	1.13	15.7	S	…	…			…	…	
539-052	2058	2	31.8	+40	55	1.23	15.6	Sb/SBc	…	…			…	…	
539-053	2060	2	31.9	+41	9	1.18	14.7	SBab	…	…	4581	1	…	…	
539-056	2066	2	32.3	+40	40	1.36	13.2	Sa	…	C:	5843	1	…	…	
Abell 400															
415-021	2372	2	51.3	+ 5	47	0.77	15.5	SAB:c	…	…	7910	1	W	D	
415-022	2375	2	51.4	+ 6	3	0.77	15.5	S	…	…	7607	1	…	…	
415-025		2	52.7	+ 5	55	0.48	15.7	S	…	(C:)	7453	1	W	VD	
415-027		2	53.1	+ 6	8	0.47	15.6	S	…	…	6760	1	…	…	
415-028	2399	2	53.2	+ 6	0	0.40	15.3	SAB:c	…	…	8006	1	…	…	
415-030	2405	2	53.3	+ 6	17	0.51	15.1	Sc	…	…	7709	1	W	D	
415-031	2414	2	53.7	+ 4	20	1.28	15.5	Sc	…	C:	8267	1	…	…	
415-032	2415	2	53.7	+ 5	57	0.29	15.5	SBbc	…	[C]	6590	1	…	…	
415-035	2419	2	54.0	+ 7	8	1.10	14.8	SBa	…	…	8090	1	…	…	
415-037	2423	2	54.1	+ 4	47	0.89	15.7	Sc	…	…	7724	1	…	…	
415-039	2426	2	54.5	+ 5	7	0.61	15.1	SA:b	…	…	7460	1	…	…	
415-042		2	55.1	+ 5	45	0.07	15.7	S: pec	D:	(C:)	7200	2	…	…	
415-048	2444	2	55.8	+ 6	6	0.28	15.2	S	…	…	6708	1	M	D	
415-053	2469	2	57.7	+ 5	31	0.62	15.2	pec:	…	(C:)	8617	1	…	…	
415-058		3	2.0	+ 5	15	1.53	15.7	Sbc:	…	…	8312	2	(W)	VD	
Abell 426															
540-036		3	2.9	+41	33	1.46	15.7	S:c: pec	D:	…	3610	2	?	?	
540-039	2534	3	3.3	+41	17	1.41	15.7	pec:	…	…	5306	1	…	…	
540-042	2538	3	3.8	+41	34	1.35	15.6	SBa	…	…	4046	1	?	?	
540-043	2544	3	4.2	+42	12	1.40	15.0	S	…	…	5198	1	…	…	
540-047	2561	3	6.4	+40	48	1.10	15.5	Sb	…	…	5821	1	…	…	
540-049	2567	3	7.0	+40	35	1.09	14.3	S-Irr	…	…	3018	1	M	VD	
540-058		3	9.9	+42	49	1.12	15.7	Sb pec	D::	…	9011	2	…	…	
525-009	2604	3	11.5	+39	27	1.26	14.8	SBc	…	…	4520	1	…	…	
540-064	2608	3	11.7	+41	51	0.53	14.0	SBb	D:	C:	7042	1	S	N	
525-011	2610	3	11.8	+39	11	1.41	15.7	Sb	…	…	5090	1	…	…	
540-065	2612	3	11.9	+41	48	0.49	15.4	Sc	…	…	6446	1	?	?	
540-067		3	12.0	+41	25	0.39	15.3	SA:a:	…	…	5945	1	M	D	
540-069	2617	3	12.7	+40	43	0.49	14.3	SABc	D::	(C:)	4627	1	M	C	
540-070	2618	3	12.7	+41	53	0.46	14.9	Sab	…	…	5376	1	W	D	
540-071		3	12.7	+42	44	0.93	15.6	SA:a:	…	…			MS	N	
540-073	2621	3	13.2	+41	21	0.25	14.7	Sa	…	…	4747	1	…	…	
540-076	2625	3	13.5	+39	50	0.96	15.7	S: pec:	…	…	4252	1	…	…	
540-078	2626	3	13.7	+41	10	0.21	15.7	Sa:	…	…	6418	2	…	…	
540-083	2639	3	14.5	+41	47	0.30	15.6	Sab	…	…	4046	1	…	…	
540-084	2640	3	14.5	+43	7	1.12	14.8	SBb	…	…	6161	1	MS	D	
540-090	2654	3	15.4	+42	7	0.49	14.6	pec:	D:	C:	5793	1	…	…	
540-091	2655	3	15.4	+43	3	1.07	14.1	SBc	…	…	6155	1	M	C	*
540-093	2658	3	15.5	+41	18	0.03	14.5	SAb	D:	(C:)	3124	1	…	…	

Table 4 – *continued*

CGCG	UGC	R.A. (1950)		Dec.		r (r_A)	m_p	Type	Dis.	Cp.	$v_\odot$ (km s^{-1})	Ref.	Hα emission Vis.	Conc.	Notes
540-094	2659	3^h	15^m.6	+40°	25′	0.57	14.9	Sbc	…	…	6193	1	S	N	
540-100	2665	3	16.2	+41	27	0.13	15.5	Sc? pec	D::	(C:)	7861	1	MW	VD	
540-103	2669	3	16.5	+41	20	0.14	13.0	pec:	…	…	5264	1	S	N	
540-106	2672	3	16.8	+40	44	0.41	15.7	Sa?	…	…	4295	1	…	…	
525-021		3	17.0	+39	23	1.24	15.5	SBa:	…	…			…	…	
540-112A	2688	3	18.0	+41	45	0.41	(15.4)	pec	D:	C	3015	1	MS	C	*
540-112B	2688	3	18.0	+41	45	0.41	(16.2)	S: pec	D	C	2882	4	?	?	*
540-114		3	18.3	+40	15	0.76	15.6	S:a:	…	…			…	…	
540-115		3	18.3	+41	19	0.35	15.6	Sa:	…	(C:)	3343	1	?	?	
540-118	2696	3	18.7	+42	0	0.57	15.7	S:	…	…	5454	1	…	…	
540-121	2700	3	19.6	+42	22	0.82	15.5	SB:b	…	…	6622	1	MW	N	
541-003		3	22.2	+40	21	1.02	14.9	SAa:	?	…			M	D	
541-005	2730	3	22.6	+40	35	0.98	15.3	Sb	…	[C:]	3772	2	…	…	
541-006	2732	3	22.8	+40	37	0.99	15.4	SBb	…	[C:]	6966	1	…	…	
541-008	2736	3	23.2	+40	20	1.12	14.7	Sab	…	…	5887	1	…	…	
541-009	2742	3	24.4	+40	44	1.14	15.5	SBc	…	…	4401	1	M	C	
541-011		3	25.2	+39	59	1.44	15.0	SB:b: pec	D:	(C:)	4246	1	S	N	
541-017	2759	3	26.7	+41	40	1.35	14.8	pec:	D:	…	4237	1	S	D	
Abell 569															
234-043	3638	6	59.2	+49	30	0.88	14.4	SB:ab	…	…	5567	1	MW	VD	
234-050	3662	7	2.1	+50	35	1.34	14.6	SBa:	…	(C::)	6276	1	…	…	
234-051	3663	7	2.1	+50	50	1.50	14.8	SBa	…	…	6290	1	…	…	
234-055		7	3.5	+48	25	0.29	15.6	S	…	…	5882	1	…	…	
234-056		7	3.8	+48	58	0.26	14.8	S pec	…	C:	6212	2	S	N	
234-057		7	4.0	+48	29	0.22	15.7	pec	…	…			M	N	
234-060	3681	7	4.3	+50	45	1.40	14.3	SBb	…	(C:)	5985	1	…	…	
234-061		7	4.4	+49	0	0.23	15.5	SAa:	…	(C::)	6236	1	W	VD	
234-062		7	4.4	+49	13	0.37	15.1	SB:a:	…	(C::)	5860	1	…	…	
234-065		7	4.7	+48	12	0.35	15.6	SB: pec	D:	(C::)			MW	VD	
234-066	3687	7	4.7	+50	42	1.37	15.5	pec:	D::	(C:)	6164	2	M	N	
234-067		7	5.0	+49	4	0.25	15.1	Sa:	…	…	6258	1	M	D	
234-069		7	5.3	+48	39	0.04	15.6	Sa:	…	C:	5296	2	W	D	
234-071		7	5.4	+49	54	0.82	15.5	SB: pec	D:	(C::)	4662	1	S	C	
234-079A	3706	7	6.1	+47	59	0.50	(15.3)	S: pec	D	C	6115	2	MS	N	*
234-079B	3706	7	6.1	+47	59	0.50	(15.7)	S: pec	D	C	6077	2	…	…	*
234-088A	3719	7	7.2	+48	35	0.22	(15.4)	Sab	D::	C	5820	2	…	…	*
234-090		7	7.2	+49	5	0.33	15.2	Sbc	…	…	5956	1	M	VD	
234-092		7	7.3	+49	58	0.89	15.7	Sa:	…	…	6296	2	…	…	
234-093	3724	7	7.7	+48	19	0.37	14.5	SBb	…	…	5925	1	MW	D	
234-094		7	7.7	+49	10	0.41	15.4	S-Irr	…	…	6089	2	W	VD	
234-100	3734	7	8.7	+47	15	1.06	13.2	SAb	…	…	955	1	…	…	
234-102		7	9.1	+49	5	0.49	15.0	Sb:	D::	(C:)			…	…	
234-103		7	9.1	+49	51	0.89	15.2	Sa:	…	…			…	…	
234-107	3741	7	10.0	+50	20	1.22	15.5	Sc	…	…	5301	1	…	…	
234-114		7	12.5	+48	21	0.84	15.6	SAa:	…	…			…	…	
235-005		7	15.1	+49	18	1.16	15.5	SA	…	…			W	VD	
235-007		7	16.8	+49	11	1.32	15.0	Sbc:	…	…			MS	VD	*
Abell 779															
180-057	4843	9	9.6	+35	7	1.49	14.2	SB	…	…	1951	1	…	…	
180-059		9	10.6	+33	31	1.10	15.7	S	…	…	3393	1	…	…	
180-060		9	10.6	+35	2	1.32	15.4	Sa:	…	…	7200	1	MW	D	
181-006	4894	9	13.7	+34	39	0.74	13.9	SB pec	D:	C:	1681	1	MW	N	*
151-048	4908	9	14.2	+32	13	1.48	15.7	Sb	…	…	14737	1	…	…	
181-007		9	14.9	+34	43	0.67	15.7	SA:a:	…	…	7002	2	…	…	
151-053		9	15.5	+32	28	1.23	15.6	SB:	…	…	8042	1	…	…	
181-012		9	15.5	+34	30	0.47	15.5	Sa:	…	…	7198	1	…	…	
181-013	4926	9	15.5	+34	46	0.66	15.4	Sb:	…	C:	6365	1	W	VD	
181-016	4935	9	16.2	+34	13	0.21	15.7	SBa	…	…	6960	1	…	…	
181-017		9	16.3	+33	57	0.09	15.3	S:a:	…	(C:)	6106	1	…	…	
181-019		9	16.4	+34	31	0.43	15.6	pec	D::	C:	13783	2	…	…	
181-023	4941	9	16.7	+33	57	0.03	15.4	S	D:	C	6106	1	W	N	
181-026	4947	9	16.9	+33	8	0.68	15.3	SB	D:	…	13790	1	?	?	
181-030		9	17.6	+33	17	0.58	15.5	SB:b	…	…	6449	1	MW	N	
181-032	4960	9	17.8	+35	35	1.29	14.8	SBb	…	…	7544	1	MW	D	
181-036		9	19.2	+34	8	0.42	15.7	S	…	(C::)	6025	1	…	…	
181-037	4988	9	20.2	+34	56	0.94	15.7	SABm	…	…	1575	1	…	…	
181-042		9	21.9	+33	57	0.85	15.6	SBbc:	…	C::	12679	2	…	…	
181-043	5015	9	22.7	+34	30	1.06	15.7	SABdm	…	…	1646	1	…	…	
181-044	5020	9	23.0	+34	52	1.24	15.3	Sc	…	C	1630	1	…	…	
181-045		9	24.2	+34	39	1.33	15.7	S:b:	…	…	6465	1	…	…	

Table 4 – *continued*

CGCG	UGC	R.A. (1950)		Dec.		r (r_A)	m_p	Type	Dis.	Cp.	$v_\odot$ (km s^{-1})	Ref.	Hα emission Vis.	Conc.	Notes
Abell 1656															
159-109	8024	12^h	51^{m}6	+27°	25′	1.24	14.9	Irr	…	…	376	2	…	…	
159-116	8033	12	52.2	+29	12	1.20	12.3	Sc	…	…	2453	1	S	N	*
160-025	8060	12	54.1	+27	15	1.00	14.0	SBa	…	(C)	6404	1	…	…	
160-038	8069	12	54.8	+29	18	0.97	14.8	SB:	D::	(C::)	7472	1	?	?	
160-043	8071	12	55.1	+28	28	0.45	15.4	S	…	C	7069	1	…	…	
160-050	8076	12	55.4	+29	55	1.40	15.2	SAB:c	…	…	5304	1	MW	VD	
160-055	8082	12	55.7	+28	31	0.37	14.2	SB:ab	D::	…	7227	1	S	N	*
160-058		12	55.8	+28	59	0.66	15.5	S	…	…	7609	1	M	D	
160-062A		12	55.9	+29	24	0.97	(15.8)	pec	D	C	7837	2	…	…	*
160-062B		12	55.9	+29	24	0.97	(15.8)	pec	D	C			…	…	*
160-064		12	56.1	+27	31	0.64	15.4	pec	D:	…	7368	1	S	N	
160-067		12	56.2	+27	26	0.70	15.4	pec	D::	…	7664	1	S	N	
160-073	8096	12	56.5	+28	6	0.20	14.9	S	…	…	7526	1	…	…	
160-075		12	56.6	+28	23	0.18	15.5	pec	D:	[C]	9386	1	M	N	
160-099		12	57.2	+28	54	0.53	15.6	Sa:	…	…	5327	1	MS	N	
160-110	8108	12	57.6	+27	10	0.88	14.7	S	…	…	5898	1	…	…	
160-113A		12	57.7	+28	8	0.11	(16.0)	pec	…	[C]	5128	2	MW	N	*
160-127		12	58.1	+27	55	0.30	15.4	pec	D::	…	7476	1	S	N	
160-130		12	58.2	+28	20	0.16	15.1	pec:	D::	…	7633	1	S	N	
160-132	8118	12	58.2	+29	17	0.85	14.6	S	…	…	7275	1	…	…	
160-139		12	58.4	+28	26	0.23	14.6	SB:ab	…	…	5807	1	…	…	
160-140	8128	12	58.5	+28	4	0.25	13.7	S	D:	C	7973	1	…	…	
160-147	8134	12	59.0	+28	8	0.30	13.7	SABa	…	…	5475	1	…	…	
160-148A	8135	12	59.0	+29	35	1.12	(15.0)	S pec	D	C	7056	1	S	VC	*
160-148B	8135	12	59.0	+29	35	1.12	(15.0)	S pec	D	C	7153	1	…	…	*
160-150		12	59.1	+28	57	0.64	15.3	S pec	D::	…	8909	1	M	D	
160-154	8140	12	59.4	+29	19	0.94	14.8	Sab	…	…	7099	1	M	D	
160-159		12	59.7	+29	31	1.11	14.9	Sa:	…	…	5823	1	…	…	
160-160		12	59.8	+28	29	0.47	15.5	pec	…	[C:]	8311	1	S	N	
160-164A		13	0.2	+28	22	0.51	(16.3)	SB:	…	C	7476	2	…	…	*
160-172	8160	13	0.9	+28	17	0.63	15.0	S:	…	(C:)	6092	1	…	…	
160-173	8161	13	1.0	+26	49	1.33	15.5	S	D:	…	6677	1	…	…	
160-176A	8167	13	1.5	+28	28	0.75	(13.5)	Sab	…	C	7111	1	…	…	*
160-178		13	2.0	+26	56	1.35	15.3	Sa:	…	…	10814	1	…	…	
160-179		13	2.0	+27	34	0.99	15.5	S: pec	D:	…	5523	1	MS	N	
160-180		13	2.0	+29	5	1.06	15.3	pec	D:	…	8050	1	S	N	
160-186	8185	13	3.3	+28	0	1.07	13.5	Sc	…	…	2533	1	MW	VD	
160-189A	8194	13	3.9	+29	20	1.45	(14.0)	S	D:	C	7135	2	…	…	*
160-191		13	4.2	+29	6	1.39	15.0	pec	D:	…	4837	1	S	N	*

References: 1. Huchra et al. (1995). 2. Nasa Extragalactic Database. 3. Moss et al. (1988). 4. Strauss et al. (1992).
Notes on individual objects:
CGCG 522-029A and B: south and north components respectively of double galaxy system.
CGCG 522-086: Emission is located ~39 arcsec west of a north–south line through the galaxy centre.
CGCG 538-043: Emission is double.
CGCG 538-056: Ring galaxy with companion 39 arcsec to east.
CGCG 540-091: Possible additional emission ~8 arcsec west of a north–south line through the galaxy centre.
CGCG 540-112A and B: north and south components respectively of double system.
CGCG 234-079A and B: south and north components respectively of double system. Interacting pair.
CGCG 234-088A: south component of double galaxy system.
CGCG 235-007: Emission has two centres.
CGCG 181-006: Ring galaxy with companion 95 arcsec to north-west.
CGCG 159-116: Emission has multiple components.
CGCG 160-055: Emission is double.
CGCG 160-062A and B: north and south components respectively of double system.
CGCG 160-113A: west component of double galaxy system.
CGCG 160-148A and B: north-east and south-west components respectively of double system. Interacting pair.
CGCG 160-164A: east component of double galaxy system.
CGCG 160-176A: west component of double galaxy system.
CGCG 160-189A: east component of double galaxy system.
CGCG 160-191: Emission is possibly double.
Explanations of columns in Table 4.
Column 1. CGCG number (Zwicky et al. 1960–1968). The numbering of CGCG galaxies in field 160 (Abell 1656), which has a subfield covering the dense central region of the cluster, follows that of the listing of the CGCG in the SIMBAD data base. The enumeration is in strict order of increasing Right Ascension, with galaxies of lower declination preceeding in cases of identical Right Ascension.
Column 2. UGC number (Nilson 1973).
Columns 3 and 4. Right Ascension and Declination (1950.0) of the galaxy centre taken from the CGCG.
Column 5. Radial distance in Abell radii (Abell 1958) of the galaxy with respect to the cluster centre. Positions of the cluster centres and values of the Abell radii for the various clusters are listed in Table 1.

Table 4 – *continued*

Column 6. CGCG photographic magnitude. For double galaxies, magnitude estimates for individual components obtained by eye from PSS are given in parentheses.
Column 7. Galaxy type taken from UGC or estimated from the PSS.
Column 8. Code indicating that the galaxy appears disturbed, on a four-rank scale (… [no disturbance], D::, D:, D).
Column 9. Code indicating that the galaxy has a possible nearby companion, on a four-rank scale (… [no companion], C::, C:, C). Square brackets indicate that the companion is likely to be a chance superposition, or has negligible tidal interaction with the galaxy; parentheses indicate that the probability of the companion being a chance superposition, $P > 0.05$ (see Section 2.3.5).
Columns 10 and 11. Heliocentric velocity and reference.
Column 12. A visibility parameter describing how readily the Hα emission is seen on the plates according to a five-point scale (S strong, MS medium-strong, M medium, MW medium-weak, W weak). A '?' in this column and column 13 indicates that the galaxy was not satisfactorily surveyed for emission for a variety of reasons: overlap by an adjacent stellar or galaxy spectrum (CGCG nos. 522-035, 522-050, 522-071, 522-082, 538-062, 540-115, 540-112B, 540-065, 540-042); overlap by a ghost image (CGCG no. 181-026); plate defect (CGCG no. 160-038); galaxy lies outside the overlap region of the plate pair (CGCG nos. 503-030, 503-044, 538-034, 540-036).
Column 13. A concentration parameter describing the spatial distribution of the emission and contrast with the underlying continuum, on a five-point scale (VD very diffuse, D diffuse, N normal, C concentrated, VC very concentrated).
Column 14. Notes. An asterisk in this column indicates that a note on this galaxy appears below the table.

by with tidal features are likely to be genuine companions (C, rank 4).

A principal difficulty in defining a robust parameter for the presence/absence of nearby companion galaxies is the uncertainty regarding projection effects — apparently close galaxies may be far apart. This is a particular problem in the crowded field of a cluster. To help overcome this problem, we use two screening criteria: one using velocity and one using local galaxy surface density.

First, if velocities were available for both the galaxy and its companion, and the absolute value of the velocity difference $|\Delta v| > 1500\,\mathrm{km\,s^{-1}}$, then it is assumed either that the projected companion is a chance superposition or, due to the high velocity difference, there is negligible tidal interaction. In either case, these galaxies were no longer considered to have 'real' companions, and were grouped with 'isolated' galaxies for the subsequent analysis. These galaxies have their companion parameters listed in square brackets in Table 4. For Abell 1367 (Paper III, table 2), galaxies CGCG nos. 97–125 and 97–133A are also in this category.

In the absence of this velocity criterion, an attempt was made to estimate the local galaxy surface density. Within an 18-arcmin box centred on the main galaxy, a count was made of the number of galaxies of a similar or greater size to the projected companion. For those cases in which the projected companion was of relatively large size such that very few, or no similar or larger galaxies were counted in the 18-arcmin box, the count was repeated for a 1-deg square box. The counts were used to estimate the mean surface galaxy density in the region, and the probability, P, was computed that the projected companion was a chance superposition (assuming that the galaxies were distributed randomly across the field). For $P > 0.05$, the sample galaxy was omitted from the companion ranking, which is given in parentheses in Table 4. For Abell 1367 (Paper III, table 2), galaxies which have been similarly omitted from the companion ranking are CGCG nos. 97-044, 97-066, 97-068, 97-120A, 127-036, 127-046, 127-085 and 127-090.

Lastly, for $P \leq 0.05$, the projected companion was accepted as a 'real' companion and assigned a rank according to the companion assignment given in Table 4.

The above procedure which selects galaxies likely to have tidally interacting companions is not quite ideal. In particular, the presence of subclustering undermines the assumption of random galaxy distribution around the main galaxy. A cleaner method would require velocity data for many fainter galaxies, which are not yet available. For the present sample, there are 36 galaxy–companion pairs with $P \leq 0.05$ and known $|\Delta v|$; of these 22 per cent have $|\Delta v| > 1500\,\mathrm{km\,s^{-1}}$. The final selected sample of galaxies with 'real' companions comprises 45 galaxies, of which some 22 have known $|\Delta v|$. Thus the contamination of the final sample by non-tidally interacting pairs is expected to be $\gtrsim$11 per cent.

3 Hα DETECTION AND GALAXY PROPERTIES

Before investigating the relation between star formation and environment, it is important first to establish the dependence of star formation on intrinsic galaxy properties. This topic has been discussed in Papers II and III. Making full use of the final galaxy survey sample, we review here in rather more detail the dependence of detected Hα emission on a variety of galaxy properties and on the presence or absence of a nearby companion. We show that the detected Hα emission can be well understood as either normal spiral disc emission, or as circumnuclear starbursts triggered either by tidal forces on the galaxy or by a bar. In at least some cases the tidal forces are due to a companion galaxy. The relation of the detected emission (whether disc emission or circumnuclear starburst) to the cluster environment of the galaxy will discussed in Section 4 below.

3.1 Apparent and absolute magnitudes

In Paper III we showed that for galaxies in Abell 1367 the Hα detection efficiency was approximately independent of apparent magnitude down to the CGCG limit, $m_\mathrm{p} = 15.7$. For our new larger sample from all eight clusters (types Sa and later, omitting irregulars or peculiars) we confirm this earlier result. Kolmogorov–Smirnov (K–S) tests which compare the cumulative distributions of apparent magnitude of non-ELGs with either compact ELGs, diffuse ELGs, or all ELGs, all show no significant differences (significance levels 0.27, 0.71 and 0.24 respectively).

Is the same true for absolute magnitude? First, we evaluated corrected magnitudes, B_T^0 following standard methods: converting CGCG magnitudes, m_p, first to the B_T system following Paturel, Bottinelli & Gouguenheim (1994), and then correcting for galactic and internal absorption following Sandage & Tammann (1987). Finally, absolute magnitudes, M_B^0, were obtained using cluster mean redshifts. Again, K–S tests which compare the cumulative distributions of absolute magnitude for non-ELGs with either compact ELGs, diffuse ELGs, or all ELGs, all show no significant differences (significance levels 0.37, 0.58 and 0.60 respectively).

Because Hα detection depends on Hubble type (though only

slightly over the range Sa to Sc; see Section 3.3 below), it is prudent to ensure that any Hubble type dependence on magnitude is not confusing these results. A more definitive test, therefore, is to compare the magnitude distribution of non-ELGs with the magnitude distribution of an 'expected' ELG sample in which each galaxy from the total sample is weighted by a Hubble type-dependent Hα detection efficiency. A comparison of this kind also shows no difference between the distributions of $m_{\rm p}$ and M_B^0 for the non-ELG and 'expected' ELG samples. We conclude that star formation rates which render a galaxy detectable in Hα are independent of absolute magnitude in the range $-22 \leq M_B^0 \leq -19$ ($H_0 = 75\,{\rm km\,s^{-1}\,Mpc^{-1}}$), and independent of apparent magnitude in the range $13 \leq m_{\rm p} \leq 15.7$ (although they drop below the CGCG limit).

These results are broadly consistent with earlier work. For example, Kennicutt & Kent (1983) found Hα equivalent widths for Sc and SBc field galaxies to be independent of absolute magnitude in the range $-22 \leq M_B \leq -17$. However, in more recent work, Gavazzi, Pierini & Boselli (1996) find an anti-correlation between Hα equivalent width and galaxy luminosity. We note that much of this trend becomes apparent only if low equivalent widths, $W_\lambda \leq 10$ Å are included, and it is not apparent for equivalent widths restricted to our detection range $W_\lambda \geq 20$ Å. Furthermore, it is possible that our photographic technique has missed fainter diffuse Hα emission in low-luminosity spirals, and this would act to mask the effect noted by Gavazzi et al.

3.2 Galaxy inclination

Does Hα detection depend on galaxy inclination? Axial ratios for our spiral sample were either taken from Nilson (1973) or measured from PSS prints (values not given in Table 4). For spirals with compact emission, a K–S test shows no significant difference between the distributions for ELGs and non-ELGs (significance level = 0.28). For diffuse emission, there is a weak tendency for highly inclined ($b/a \lesssim 0.3$) galaxies to be less easily detected, but the effect is only marginal (significance level = 0.06). These results are encouraging, partly because galaxy inclination can be ignored in our subsequent analyses, and partly because both nuclear and disc emission are unlikely to be masked unless the galaxy is almost edge-on.

3.3 Hubble type

In Fig. 2 we show the percentage detection of ELGs for the full range of Hubble types. Data for early-type galaxies (E, E-S0, S0 and S0/a) are for Abell 1367 (Paper III), and data for the remaining types are for all eight clusters. The figure shows a trend of increasing star formation rate per unit luminosity from early-type to later type galaxies, which is well known from previous Hα, UV and FIR studies (Kennicutt 1998).

How do our observed percentage detections of ELGs over the range of Hubble types using the prism survey compare with percentages we might expect to detect based on previous photoelectric and CCD photometry? To answer this question, we have constructed a comparison sample of galaxies with photoelectric and CCD measurements of Hα+[N II] equivalent width, by combining data given by Kennicutt & Kent (1983), Romanishin (1990) and Kennicutt (1992). In order that the sample be representative of the field, low surface brightness galaxies, Markarian and Seyfert galaxies, and galaxies from Coma and

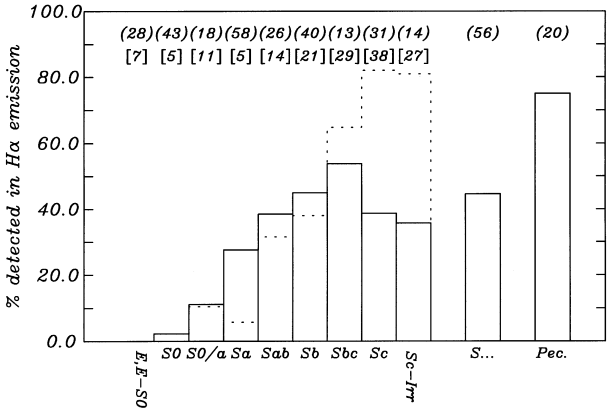

Figure 2. The percentage detection of Hα + [N II] emission for galaxies in different Hubble type bins (solid histogram). The total sample number for each bin is given in parentheses. Also shown are expected percentage detections for bins in the range E to Sc–Irr (dotted histogram) based on a sample of field galaxies observed using photoelectric and CCD photometry. The total field galaxy sample number for each bin is given in square brackets.

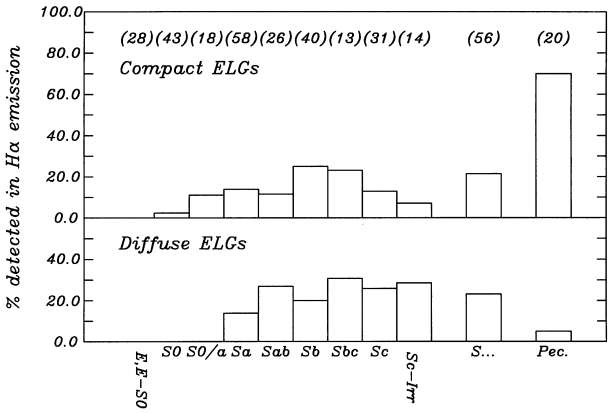

Figure 3. (Upper panel) The percentage detection of compact Hα + [N II] emission for galaxies in different Hubble type bins. (Lower panel) As upper panel, for diffuse emission. The total sample number for each bin is given in parentheses.

Abell 1367 were omitted from the sample. To match our cluster galaxies, the sample was further restricted in absolute magnitude to $M_B^0 \leq -19$. In Paper III we established an overall efficiency for the objective-prism technique by comparing its results with photoelectric observations of galaxies in Abell 1367 and 1656: ~90 per cent complete for $W_\lambda \geq 20$ Å and ~29 per cent complete for $W_\lambda \leq 20$ Å. Assuming these detection efficiencies, we derive expected ELG detections by the prism survey for the comparison sample in the range E to Sc–Irr.

Note that since we use de Vaucouleurs types for the cluster galaxies, we also use RC3 (de Vaucouleurs et al. 1991) types for the comparison sample, following the cautionary statements by Hameed & Devereux (1999), who note that systematic type differences between the RC3 and the RSA classification schemes (i.e., those of de Vaucouleurs and Sandage) may lead to systematic differences in the inferred dependence of star formation on Hubble type.

The dotted histogram in Fig. 2 shows the predicted fraction of detected galaxies for the comparison sample. The detection rate for early-type spirals is similar to that predicted (χ^2

significance = 0.5 for S0/a–Sb), but there are fewer late-type ELGs detected than expected (χ^2 significance = 6×10^{-6} for Sc and later). It is not immediately clear how to interpret this. One possibility is that there is reduced star formation in late-type spirals in clusters, but since our later analysis fails to find this effect (see Section 4.3), we instead suspect that the photographic technique is in fact less efficient in detecting diffuse emission in late-type spirals. We note that in Paper II we found a similar result with similar ambiguous interpretation, while in Paper III there were too few late-type galaxies to attempt a meaningful comparison. Further work is in progress to better test the detection efficiency of the prism survey.

In Fig. 3 we compare the Hubble type distribution for detection of compact ELGs (upper panel) and diffuse ELGs (lower panel). Several features of this figure and the previous figure may be noted. First, the morphological class with the highest Hα detection rate (~75 per cent) are 'Peculiar' galaxies, and the detections are almost exclusively compact emission. In Section 3.6 below, we suggest that many of these peculiar galaxies are ongoing mergers with associated nuclear starbursts. Second, the large but poorly defined class of 'S…' galaxies has Hα detection rates in each category (all, compact, diffuse) which closely match those of the 'typed' spirals. This supports their inclusion with the rest of the spirals in the subsequent analysis. Finally, the small fraction of early-type galaxies (S0,S0/a) detected in Hα all have compact emission, matching the findings of Bennett & Moss (1998) for three early-type galaxies in Abell 1060. This suggests a tidal or post-merger origin for the emission in these systems (see Section 4).

3.4 Bars

Does the presence of a bar influence star formation? For the 128 galaxies with bar information, Kendall rank tests yield 0.3σ, 3.6σ and -3.2σ for correlation strengths between the presence of a bar and the emission-line categories ELG(all), ELG(compact), ELG(diffuse) respectively. Thus it seems that barred galaxies are more likely to have compact emission than unbarred spirals, but less likely to have diffuse emission. While spiral stage is not expected to influence these correlations (because there is no significant dependence of bars on spiral stage), galaxy disturbance may influence them, since compact emission and disturbance are strongly linked (see below). Accordingly, we have calculated the corresponding partial rank correlation coefficients for the case in which galaxy disturbance is partialled out, and estimated their significance levels using a bootstrap resampling technique provided by Biviano (private communication). The resulting significance levels are 0.7σ, 3.1σ and -3.0σ for correlation strengths between the presence of a bar and the emission-line categories ELG(all), ELG(compact), ELG(diffuse) respectively. These results confirm, in agreement with Paper III, that while there is no overall enhancement of emission in barred spirals, they tend to have compact emission. The same results indicate that unbarred spirals tend to have diffuse emission, although this may at least partly be due to the presence of diffuse emission on the prism plates being overlooked for a number of galaxies due to the dominance of compact emission.

3.5 Disturbance

For the full cluster sample, a Kendall rank test between disturbance and the emission-line categories ELG(all), ELG(compact), ELG(diffuse) gives correlation significances of 5.4σ, 8.7σ and -2.2σ respectively. As noted above (Section 3.3), most galaxies classified as peculiar also have compact emission. Omitting these types leaves a sample of 270 spirals for which a Kendall rank test shows similar correlations: 4.4σ, 7.5σ and -1.6σ respectively. Thus a disturbed galaxy morphology is a strong predictor of compact emission. This correlation is the more striking, since indications of a disturbed morphology are generally taken from the *outer* features of the galaxy. The obvious explanation for this correlation is tidally induced star formation, which is discussed further in Section 3.7 below. These results for the full sample echo our previous work in Papers II and III with more limited samples.

3.6 Galaxy companions and mergers

Although a Kendall rank test for the companion parameter with emission yields no significant result for the combined sample of all ELGs (significance of -0.3σ), there are significant correlations in opposite senses for compact and diffuse emission taken separately (significances of 3.1σ and -3.5σ respectively). The exclusive tendency for compact ELGs to have tidal companions further confirms an explanation of tidally induced star formation for much of this emission, some of which is caused by local galaxy–galaxy interactions.

On the other hand, as noted above (Section 3.3) a very high percentage (~70 per cent) of galaxies classified as peculiar have compact emission. However, these galaxies show no tendency to have tidal companions (Kendall rank test significance = 1.4σ). A natural explanation of these results is that the peculiars are predominantly ongoing mergers, in which the companion is already indistinguishable from its merger partner. These then represent a later stage of close double, interacting systems, many examples of which are found in the clusters with tidally induced star formation (e.g., CGCG nos. 540-112, 234-079, 127-025, 97-079, 97-092, 127-051, 160-113 and 160-148). For the remaining sample of spiral galaxies alone, a Kendall rank test shows an even stronger correlation between the companion parameter and compact emission (significance of 4.6σ) consistent with this picture.

Interestingly, there is an *anticorrelation* between diffuse Hα emission and a tidal companion, although, as for the observed anticorrelation of diffuse emission and the presence of a bar (see Section 3.4), this may at least partly be due to the presence of diffuse emission being overlooked in cases where compact emission is dominant.

3.7 Starburst and disc emission

Kennicutt (1998) notes that large-scale star formation takes place in two very distinct physical environments, viz. in the extended discs of spiral and irregular galaxies, and in compact, dense gas discs in the centres of galaxies. Line emission associated with star formation in the two regions has very different dependencies on galaxy morphology. In particular, circumnuclear emission has a strong dependence on a barred structure but weak dependence on Hubble type, while the opposite is true for disc emission. In addition, a clear causal link between strong nuclear starbursts and tidal interactions and mergers has been established by numerous observations (e.g. Keel et al. 1985; Bushouse 1987; Kennicutt et al.

1987; Wright et al. 1988) consistent with predictions of numerical simulations (e.g. Noguchi 1988; Hernquist 1989; Mihos & Hernquist 1996). For nearby samples of interacting galaxies, the Hα emission is typically 3–4 times stronger than for isolated spirals.

In view of the above, the obvious and most compelling interpretation of the distinction between compact and diffuse emission in our survey sample is that of circumnuclear starburst and disc emission respectively. As has been seen, compact emission is generally centred on the nucleus of the galaxy and is of smaller spatial extent (median diameter $\sim$2.5 kpc, Paper II), and correlates with a barred structure, all of which is typical of circumnuclear emission. Furthermore, compact emission is strongly correlated with a disturbed morphology and with the presence of a nearby companion, strongly suggesting that much of this emission is indeed due to tidally induced nuclear starbursts. Finally, there is no significant dependence of compact emission on Hubble stage from Sa–Sc. By contrast, diffuse emission has a greater spatial extent closer to that expected for disc emission (median diameter $\sim$7 kpc; Paper II) and is not correlated either with a barred structure or a disturbed morphology. There is no apparent dependence of emission on Hubble stage, but this is not considered significant because of uncertainties associated with detection of diffuse emission (cf. Section 3.3).

Despite the above considerations, could the compact emission be due to non-stellar emission? Ho, Filippenko & Sargent (1997a) have extended earlier studies to show that AGN and LINER (Heckman 1980) emission is very common, particularly in early-type spirals, of which 60 per cent show this non-stellar activity. However, galaxies in their sample have low Hα luminosity (median $L_{\rm H\alpha} \sim 10^{39}\,{\rm erg\,s^{-1}}$). By contrast, the H$\alpha$ luminosities of the ELGs in our survey sample are higher ($10^{40} \lesssim L_{\rm H\alpha} \lesssim 5 \times 10^{41}\,{\rm erg\,s^{-1}}$), more typical of lower luminosity starburst emission (Balzano 1983). Moreover, Ho, Filippenko & Sargent (1997b) show that whereas bars enhance nuclear star formation in their sample, there is no corresponding enhancement of AGN activity. Finally, despite the fact that a few of our ELGs are classed as Seyferts (viz. CGCG nos. 126-110, 522-081, 540-064, 540-103 and 160-148A) a spectral survey of ELGs in Abell 1367 (Moss & Whittle, unpublished) has confirmed that emission for most of these galaxies resemble H II regions and not AGN or LINERs. For these reasons, it is considered unlikely that most compact emission has a non-stellar origin. In what follows, we assume that both compact and diffuse emission are due to photoionization by massive young stars, and investigate how the corresponding circumnuclear starburst and disc star formation varies within a cluster and field environment.

4 Hα DETECTION AND CLUSTER ENVIRONMENT

4.1 Introduction

Using the full sample of surveyed galaxies, we compare emission detection rates in cluster and field spirals in a manner which overcomes three principal limitations of earlier studies (Papers II and III). First, we observe our own field sample in an identical manner to the cluster sample, unlike our earlier work which used a field sample observed by photoelectric photometry, possibly introducing systematic biases. Second, our field sample is greatly enlarged from that used for Paper III. Third, whereas in Paper III we made the cluster/field comparison for only a single cluster, here we make use of the entire survey sample which includes a full range of cluster types.

Before proceeding to the comparison, it is first necessary to consider how this may be affected by the use of Hubble types and by field galaxy contamination.

4.1.1 Hubble type and bulge/disc ratio in cluster/field comparisons

We have chosen to use Hubble types to normalize galaxy samples when comparing cluster and field galaxies. Several authors have noted that the Hubble classification system was based mainly on nearby field spirals and may not be adequate to describe environmentally altered galaxies in dense environments (e.g. van den Bergh 1976, 1997; Koopmann & Kenney 1998). In particular, one characteristic used to determine Hubble type is the resolution of the spiral arms, which is itself related to star formation. Thus, for example, a decrease in the disc star formation which also shifts a galaxy to an earlier Hubble type may not be detected in any comparison of field and cluster spirals (Hashimoto et al. 1998).

Some authors (e.g. Balogh et al. 1998; Hashimoto et al. 1998) have instead adopted a measure of bulge to disc ratio (B/D) as a less subjective and star formation-contaminated normalization parameter. However, the use of B/D ratio may introduce other problems. First, the relation between B/D and Hubble T-type has sufficient scatter (Simien & de Vaucouleurs 1986; de Jong 1995; Baugh, Cole & Frenk 1996) that a galaxy with $\mathrm{B/D} = 1$, for example, could lie anywhere in the range S0–Sbc. It is still not known whether the scatter in the relation is observational or real (Baugh et al. 1996). Second, because of this scatter in the B/D versus T-type relation, S0 galaxies will be included in both field and cluster samples, and so an increase in the S0/S ratio in clusters can lead to a perceived reduction in star formation rate. Thirdly, the B/D ratio itself may depend on star formation. A change in star formation rate in either the disc and/or the circumnuclear regions will change the B/D ratio (Balogh et al. 1998).

Thus, although there may be no better alternative to using the Hubble type for cluster/field comparison, the use of Hubble types introduces a possible limitation to our study, at least for *disc* emission. In what follows, we find no difference between disc emission in field and cluster samples. It remains unclear to what extent this result may represent a limitation of the method, rather than a true comparison of the two samples. By contrast, we do expect a comparison based on Hubble type to be sensitive to differences of *circumnuclear* star formation. Such star formation has little or no relation to Hubble type (Kennicutt 1998) and, consistent with this, is not expected to affect the type classification.

4.1.2 Sample contamination by field galaxies

Any comparison of cluster and field galaxies needs to allow for possible contamination of the cluster sample by projected field galaxies. This contamination is more severe for late-type galaxies (such as our own sample) than early-type galaxies because late-type galaxies are less common in clusters than in the field.

We have attempted to estimate the contamination effect on our cluster spiral sample for a series of concentric zones for all eight clusters (see below). The estimates are useful in several ways. First, they confirm that contamination by field projection is not important, at least in the cluster centres and for regions of high galaxy surface density. Second, the estimates can be used to select zones for a true comparison of cluster and field samples. Finally,

Table 5. Field galaxy contamination of cluster spiral sample.

Cluster	Zone 1 (0.0–$0.5r_A$)			Zone 2 ($0.5r_A$–$1.0r_A$)			Zone 3 ($1.0r_A$–$1.5r_A$)			Zone 4 ($1.5r_A$–$3.0r_A$)
	n_s	n_{fs}	p_{fs}	n_s	n_{fs}	p_{fs}	n_s	n_{fs}	p_{fs}	n_t
Abell 262	16	4	22 per cent	25	11	42 per cent	16	18	[100 per cent]	155
Abell 347	15	3	18 per cent	12	8	67 per cent	13	13	[100 per cent]	119
Abell 400	6	1	15 per cent	6	3	45 per cent	2	5	[100 per cent]	40
Abell 426	14	2	13 per cent	9	5	61 per cent	17	9	54 per cent	81
Abell 569	14	2	12 per cent							77
Abell 569N	6	2	29 per cent							77
Abell 779	6	1	21 per cent	7	4	54 per cent	9	6	70 per cent	56
Abell 1367	19	3	17 per cent	9	10	[100 per cent]	20	16	80 per cent	141
Abell 1656	11	2	15 per cent	14	5	34 per cent	12	8	67 per cent	71

Table 6. Cluster zonal space densities.

Cluster	n_1	n_2	n_3	d_1	d_2	$>d_3$	ρ_1	ρ_2	ρ_3
				(r_A^{-3})			(Mpc^{-3})		
Abell 262	44	45	23	54.7	10.2	0.0	2.10	0.39	0.00
Abell 347	23	24	21	28.4	4.0	0.0	1.62	0.23	0.00
Abell 400	16	9	3	24.7	1.7	0.0	3.09	0.21	0.00
Abell 426	41	27	36	62.8	2.3	3.6	3.76	0.14	0.21
Abell 569	24			40.4			2.30		
Abell 569N	24			40.4			2.30		
Abell 779	19	15	9	26.5	3.1	0.0	1.68	0.20	0.00
Abell 1367	67	21	35	115.4	0.1	1.5	7.39	0.01	0.10
Abell 1656	85	62	37	122.6	15.7	4.1	10.72	1.30	0.35

the space density of the central zone of each cluster can be used to rank the clusters for tests of the dependence of emission and other galaxy properties on cluster type.

We estimate field contamination as follows. First, for each cluster (except Abell 569 which is double), we consider four concentric annular zones, 1–4: $0.0 - 0.5r_A$; $0.5r_A - 1.0r_A$; $1.0r_A - 1.5r_A$; and $1.5r_A - 3.0r_A$, where r_A is the Abell radius. We assume that all galaxies in the outermost annulus, $1.5r_A - 3.0r_A$, are field galaxies. For each cluster, Table 5 gives the total number of spirals, n_s, in zones 1–3, and the total number of galaxies of *all* types, n_t, in the outermost zone. For Abell 569 the principal component is situated at the cluster centre, and a secondary component lies approximately $1^\circ.5$ north. Values of n_s are given only for regions of radius $0.5r_A$ centred on each of the two subclusters.

First, we need an estimate of the spiral fraction in zone 4, since most CGCG galaxies in this zone have not been typed. As shown below (see Table 6), the true space density (i.e., after field correction) in zone 3 for each of the four least rich clusters (Abell 262, 347, 400 and 779) is essentially zero. Thus galaxies in these zones can be considered as projected (supercluster) field galaxies. From these zones, and a total of 78 typed CGCG galaxies in zone 4 of Abell 1367 (cf. Paper III), we measure a spiral fraction of 61 per cent. This value was adopted for the spiral fraction for zone 4 of all the clusters, and used to estimate the number of projected field spirals, n_{fs}, and the percentage contamination, p_{fs}, for zones 1–3 in each of the clusters (see Table 5).

Note that although there is considerable contamination for zone 3 (outside the nominal limit of the clusters), and significant contamination for zone 2 for most of the clusters ($p_{fs} \gtrsim 50$ per cent), in zone 1 the contamination is generally low ($p_{fs} \sim 17$ per cent). This gives us confidence that a valid comparison is possible between cluster and field spirals in the survey sample, at least for this central zone.

Next, following a procedure similar to that of Wallenquist (1960) and assuming spherical symmetry for the cluster and uniform density within each annulus, the apparent space densities, d_1, d_2, and d_3 in each zone in units of galaxies r_A^{-3}, are given by:

$$d_3 = \frac{n_3^c}{\frac{4}{3}\pi(r_3^2 - r_2^2)^{\frac{3}{2}}}$$

$$d_2 = \frac{n_2^c - Xd_3}{\frac{4}{3}\pi(r_2^2 - r_1^2)^{\frac{3}{2}}}$$

$$d_1 = \frac{n_1^c - Yd_3 - Zd_2}{\frac{4}{3}\pi r_1^3},$$

where

$$X = \tfrac{4}{3}\pi(r_3^2 - r_1^2)^{\frac{3}{2}} - \tfrac{4}{3}\pi(r_3^2 - r_2^2)^{\frac{3}{2}} - \tfrac{4}{3}\pi(r_2^2 - r_1^2)^{\frac{3}{2}}$$

$$Y = \tfrac{4}{3}\pi r_3^3 - \tfrac{4}{3}\pi(r_3^2 - r_1^2)^{\frac{3}{2}} - \tfrac{4}{3}\pi r_2^3 + \tfrac{4}{3}\pi(r_2^2 - r_1^2)^{\frac{3}{2}}$$

$$Z = \tfrac{4}{3}\pi r_2^3 - \tfrac{4}{3}\pi r_1^3 - \tfrac{4}{3}\pi(r_2^2 - r_1^2)^{\frac{3}{2}},$$

and n_1^c, n_2^c and n_3^c are the total numbers of CGCG galaxies of all types in zones 1, 2 and 3 respectively, corrected for projected field galaxies. Taking $r_1 = 0.5$, $r_2 = 1.0$ and $r_3 = 1.5$, we have $X = 3.2730$, $Y = 0.8214$ and $Z = 0.9445$, which yield the apparent space densities given in Table 6. For the double cluster Abell 569 we have adopted a simplified procedure. The galaxy count for zone 1 for the two cluster components was corrected only for projected field galaxies, and the resulting corrected count was used to determine values of d_1 given in the table.

The apparent space densities are not directly comparable, because the magnitude limit of the CGCG catalogue, $m_p = 15.7$, corresponds to different absolute magnitude limits, M_B, depending on cluster distance modulus and Galactic reddening. Using the

conversion of m_p to absolute magnitude given in Section 3.1, and adopting a common limit, $M_B \lesssim -19.5$, we obtain the true space densities, ρ_1, ρ_2, ρ_3 (in units of galaxies Mpc^{-3}; see Table 6). These space densities will be used for the ranking of clusters in Section 4.2.3 below.

4.2 Cluster/field parameters

We have used three parameters to compare the incidence of star formation in clusters and field spirals: projected radial distance from the cluster centre, R; local galaxy surface density, Σ; and cluster type, *CT*, determined by the central galaxy density. These parameters are, of course, closely related: Σ and *CT* are strongly correlated, while R and Σ are strongly anticorrelated. Before using these parameters (see Section 4.3), we briefly define them.

4.2.1 Projected radial distance from cluster centre, R

Using the projected radial distance, R, for each surveyed galaxy, measured in Abell radii, galaxies in each of the surveyed clusters (except the double cluster Abell 569) were stacked into a single 'synthetic' cluster. For the purpose of Kendall rank tests, the survey sample was divided into 10 radial bins, each with approximately equal populations ($n \sim 32$).

Use of the radial distance parameter has obvious limitations. The method neglects azimuthal variations in galaxy density, as well as systematic variations in cluster properties. Nevertheless, any systematic change in emission properties of spirals from the field to a cluster environment might be expected to show a systematic change with R.

4.2.2 Local galaxy surface density, Σ

To define a local galaxy surface density parameter, Σ, we follow the procedure used by Dressler (1980). First, for each surveyed galaxy, the 10 nearest projected CGCG neighbours are identified, and the distance to the tenth nearest defines the radius of a circle. After correction for field galaxy contamination, the galaxy surface density in this circle is calculated. If the estimated number of projected field spirals in the circle is ≥ 10, the surface density is set to zero. A correction is made for the different absolute magnitude limits of the galaxy counts for each cluster. The final value of the local surface density, Σ, is the number of galaxies, $M_B \leq -19.5\,\mathrm{Mpc}^{-2}$. For the purpose of Kendall rank tests, surveyed galaxies were divided into discrete bins covering the range of Σ. Galaxies with values of $\Sigma = 0$ were gathered in one bin ($n = 132$), and remaining galaxies were grouped in nine bins according to surface density with approximately equal populations ($n \sim 21$).

4.2.3 Cluster type, CT

We have ranked each cluster according to its central galaxy space density, ρ_1, defined as the mean space density of galaxies, $M_B \leq -19.5\,\mathrm{Mpc}^{-3}$ within the central region $r \leq 0.5 r_A$ (see Table 6). In addition, we assign the lowest rank to field (supercluster) spirals which comprise surveyed galaxies with $r > 1.5 r_A$ together with those in zone 3 of Abell 262, 347, 400 and 779 (see Section 4.1.2 above). Cluster galaxies were taken as those surveyed galaxies with $r \leq 1.0 r_A$. Ranks were assigned as follows: rank 1, field spirals as above; rank 2 ($\rho_1 \sim 2\,\mathrm{Mpc}^{-3}$), Abell 262, 347, 569 and 779; rank 3 ($\rho_1 \sim 3\,\mathrm{Mpc}^{-3}$), Abell 400; rank 4 ($\rho_1 \sim 4\,\mathrm{Mpc}^{-3}$), Abell 426; rank 5 ($\rho_1 \sim 7\,\mathrm{Mpc}^{-3}$), Abell 1367; and rank 6 ($\rho_1 \sim 11\,\mathrm{Mpc}^{-3}$), Abell 1656.

4.3 Comparison of emission detection rates for different environments

In considering the dependence of emission detection rates on different environments using the parameters R, Σ and *CT* defined above, we need to ensure that any significant correlations which arise are not spuriously due to indirect dependencies on other variables. To assess this, we first consider Kendall rank tests between these three parameters and several possibly relevant galaxy properties, viz. Hubble type, bar, disturbed morphology, and the incidence of galaxies classified as peculiar. For these tests (and subsequent tests of emission detection rates on environment), the sample was restricted to galaxies whose known radial velocity was not greater than 3σ from the cluster mean. Results of these tests are given in Table 7. For this, and Tables 8 and 9 below, test results are given as the significance in units of σ with the sample number in parentheses.

First, it is seen that, as noted above, there is no significant correlation between Hubble stage and either R or Σ, and a possible weak anticorrelation with *CT*. Thus, in considering systematic correlations of emission detection rate with either R or Σ, the effect of Hubble stage can be neglected. For the parameter *CT*, the effect of the systematic variation of Hubble stage is to decrease the likelihood of emission for cluster as compared to field galaxies. However, in what follows, we are concerned with an *increase* of emission detection for cluster galaxies, and the effect of Hubble stage is thus to make this increase even more significant.

Second, it is seen that there is no significant correlation of a barred structure with either R, Σ or *CT*. In Section 3.4 above, it was noted that there is a correlation of compact emission with a barred structure. Below, we will note a strong enhancement of compact emission for cluster as compared to field spirals. The lack of correlation between barred structure and a cluster environment shows that the enhanced compact emission cannot be due to an increase in barred structure in cluster spirals.

Next, the results show a possible weak correlation of a disturbed morphology with local galaxy surface density. This effect can most simply be attributed to enhanced tidal effects on spirals in higher density regions.

Finally, it is seen that peculiar galaxies are more likely to be

Table 7. Kendall rank tests: cluster/field and galaxy properties.

	Spirals only						Peculiar	
	Hubble stage		Bar		Disturbed morphology		type	
R	0.6σ	(148)	1.6σ	(107)	-1.4σ	(235)	-1.3σ	(257)
Σ	−0.5	(148)	−0.3	(107)	2.2	(235)	1.9	(257)
CT	−2.2	(124)	−1.4	(86)	1.5	(194)	3.8	(210)

Table 8. Kendall rank tests: cluster/field and emission detection.

	All sample						Spirals only					
	ELGs (all)		ELGs (compact)		ELGs (diffuse)		ELGs (all)		ELGs (compact)		ELGs (diffuse)	
R	-1.0σ	(257)	-2.6σ	(257)	1.4σ	(257)	-2.4σ	(237)	-1.9σ	(237)	-1.1σ	(237)
Σ	2.6	(257)	3.9	(257)	-0.7	(257)	1.8	(237)	2.5	(237)	-0.2	(237)
CT	3.2	(210)	5.3	(210)	-1.3	(210)	2.3	(195)	4.0	(195)	-0.8	(195)

Table 9. Kendall rank tests: cluster/field spiral subtypes and emission detection.

	Sa,Sab						Sb,Sbc						Sc–Irr					
	ELGs (all)		ELGs (compact)		ELGs (diffuse)		ELGs (all)		ELGs (compact)		ELGs (diffuse)		ELGs (all)		ELGs (compact)		ELGs (diffuse)	
R	-1.1σ	(83)	-2.6σ	(83)	0.9σ	(83)	1.0σ	(53)	-0.9σ	(53)	2.1σ	(53)	-1.8σ	(45)	-1.3σ	(45)	-1.1σ	(45)
Σ	1.8	(83)	1.9	(83)	0.5	(83)	-0.7	(53)	1.2	(53)	-2.0	(53)	1.7	(45)	1.2	(45)	1.0	(45)
CT	2.7	(68)	4.3	(68)	-0.3	(68)	0.0	(42)	2.5	(42)	-2.6	(42)	3.2	(37)	3.3	(37)	1.4	(37)

found in higher surface density regions and in richer clusters. Since a large percentage of these galaxies ($\sim$70 per cent) show compact emission, a corresponding increase of compact emission in the cluster sample as compared to the field is to be expected.

In Table 8 we give Kendall rank test results for emission in the three categories, ELGs(all), ELGs(compact) and ELGs(diffuse) with each of the parameters R, Σ and CT. Since for these results and subsequent results, given in Table 9, the most significant correlations are found for Σ and CT, we will discuss these. Results for the parameter R are generally indicative of similar effects found by the other two parameters, but are much weaker and accordingly of less interest.

From Table 8 it is seen that there is a significant correlation of emission detection rate with CT (significance level, 3.2σ) and some suggestion of such a correlation with Σ (significance level, 2.6σ). Galaxies of types Sa and later thus are more likely to have emission in clusters with higher than lower central density. This result is a surprising one, and the opposite of that expected on the basis of cluster spiral gas content, and its significance is perhaps even greater than the test results indicate, due to a weak correlation of Hubble stage with cluster density which contributes to lowering the emission detection rate for galaxies in the most dense clusters.

Furthermore, the correlation of emission detection rate with Σ and CT is seen to be entirely due to a very significant correlation of compact emission with these parameters (3.9σ and 5.3σ respectively). This enhancement of compact emission in cluster galaxies as compared to the field is not due simply to an increased likelihood of 'peculiar' galaxies being found in the cluster environment. In Table 8 we show Kendall rank test results between ELGs(all), ELGs(compact) and ELGs(diffuse) and R, Σ and CT for the spiral sample alone (excluding galaxies classed as 'peculiar'). There is a similar correlation of emission detection rate with both Σ and CT, as for the full sample, and the increase in emission in regions of higher density and for clusters of higher central density is again seen to be entirely due to enhanced compact emission. As noted above, the enhanced compact emission in cluster spirals cannot be due to an increase in a barred structure for these galaxies. Rather, we conclude that it is due to low-luminosity circumnuclear starbursts due to increased tidal interactions in the cluster environment. This view is supported by the fact that a Kendall rank test shows that both the most disturbed spirals and peculiar galaxies are preferentially found in clusters of higher central density (significance levels of 3.2σ and 3.8σ respectively).

The enhancement of compact emission in cluster as compared to field spirals has been shown from the correlation of the emission detection rate with both local galaxy surface density and with cluster type, ranked according to central galaxy density. Is the emission enhancement entirely due to local galaxy surface density, with the observed correlation with cluster type simply due to a greater proportion of galaxies in the more dense clusters being situated in regions of higher surface density? Or is there a 'cluster effect', such that galaxies in a region of a given surface density in more dense clusters, are more likely to have compact emission than galaxies in a region of the same surface density in less dense clusters? A Kendall partial rank test of the correlation of compact emission with cluster type for the case in which local galaxy surface density is partialled out yields a significance level $= 3.3\sigma$. It thus appears that there is indeed a 'cluster effect', and that galaxies in a region of a given surface density in a more dense cluster are more likely to have compact emission than galaxies in a region of the same surface density in a less dense cluster. The implications of this result will be discussed further in Section 5 below.

In Table 9 we give results of Kendall rank tests between ELGs(all), ELGs(compact) and ELGs(diffuse) and R, Σ and CT for the spiral subgroups, Sa and Sab, Sb and Sbc, and Sc–Irr. It is seen that for each of the subgroups, there is the same increase of compact emission with higher surface density regions and more dense clusters as for the full sample of spirals combined. Of particular interest is the very significant correlation of emission detection rate with increasing cluster density for Sc–Irr galaxies. In Section 3.3 it was seen that surveyed spirals of these types have a lower detection rate than expected from photoelectric and CCD photometry. We can conclude that it is unlikely that this lower detection rate is due to any lessened emission from cluster as compared to field spirals. Rather, it is more likely, as previously suggested (Section 3.3), that this lower detection rate is due to non-detection of diffuse disc emission in the low surface brightness discs of these galaxies by the photographic survey. Work is in progress to verify this conclusion.

5 DISCUSSION

The analysis of the full cluster sample confirms earlier conclusions (Papers II and III) that there is an enhancement of tidally

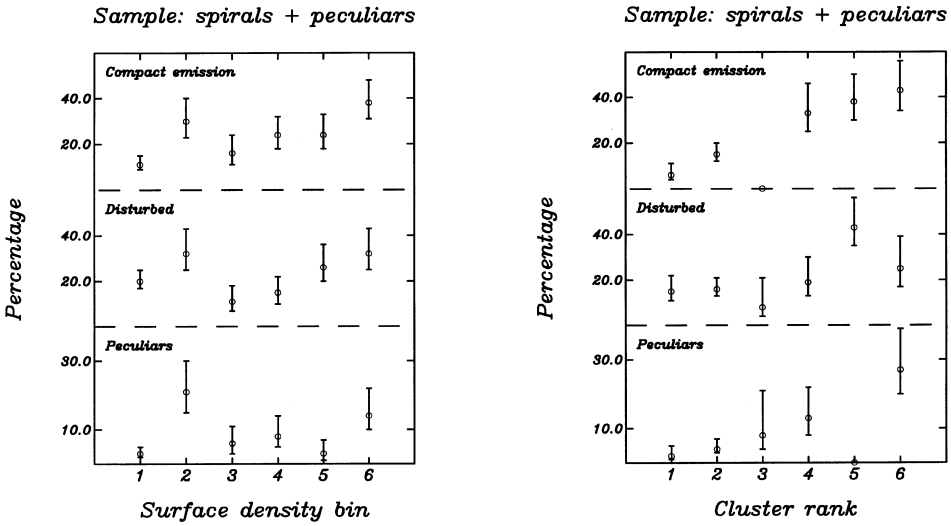

Figure 4. (Left-hand panel) Percentages of galaxies which have compact emission, are disturbed or are classified as peculiar, with increasing local galaxy surface density, Σ. The surface density bins, 1–6, correspond to median values of Σ equal to 0.0, 0.3, 1.0, 2.3, 4.9 and 14.4 galaxies, $M_B \leq -19.5$, Mpc^{-2} respectively. (Right-hand panel) As left-hand panel, with increasing cluster central galaxy space density. Cluster ranks are as follows: rank 1, field spirals; rank 2 ($\rho_1 \sim 2\,\mathrm{Mpc}^{-3}$), Abell 262, 347, 569, 779; rank 3 ($\rho_1 \sim 3\,\mathrm{Mpc}^{-3}$), Abell 400; rank 4 ($\rho_1 \sim 4\,\mathrm{Mpc}^{-3}$), Abell 426; rank 5 ($\rho_1 \sim 7\,\mathrm{Mpc}^{-3}$), Abell 1367; and rank 6 ($\rho_1 \sim 11\,\mathrm{Mpc}^{-3}$), Abell 1656. The galaxy sample for both panels comprises galaxies classified as spiral or peculiar.

induced circumnuclear star formation in cluster galaxies (types Sa and later) compared to similar galaxies in the field. Whereas previous work established this simple contrast, the current work shows that the frequency of circumnuclear starbursts is consistent with a monotonic increase with increasingly dense cluster environments. Fig. 4 shows the increase in the fraction of spirals with compact emission with cluster rank, from the field (rank 1) to the richest cluster (Coma, rank 6), as well as with increasing local galaxy surface density, Σ. In particular, we do *not* confirm the result from Hashimoto et al. (1998), who found that poor clusters have higher levels of starburst emission than either the field environment or rich clusters. In fact, the proportion of spirals with compact emission increases dramatically from the field (~8 per cent) to the richest cluster (Coma; ~43 per cent). There are corresponding increases in the fractions of spirals classed as peculiar (~2 per cent in the field; ~35 per cent in Coma) and those noted as disturbed (~11 per cent in the field; ~39 per cent and 25 per cent in Abell 1367 and Coma respectively).

Is it possible to integrate these findings into a broader picture; one which addresses cluster evolution from intermediate redshifts to the present? Obviously, in a rich cluster such as Coma the residual spiral fraction is much smaller than the spiral fractions in similar clusters at intermediate redshift. However, it appears from our study that *the residual spiral population in nearby rich clusters is similar to the spiral population in clusters at intermediate redshift*. The Butcher–Oemler effect would appear to be mainly due to a *decrease* in the spiral population over the last few giga-years, not primarily a change in the properties of spirals themselves. The fraction of spirals in Coma which are peculiar, showing signs of interaction and distortion, and which are undergoing tidally induced star formation appears similar to the fraction of spirals which show these effects in rich clusters at $z \sim 0.5$. Yet further evidence that tides and interactions are important in nearby clusters and not just in distant clusters has been given by Conselice & Gallagher (1999). These authors detect a variety of unusual fine-scale substructures, including distorted and interacting galaxies, in five nearby clusters which they consider to be caused by tidal forces. Trentham & Mobasher (1998) have discovered a giant low-surface-brightness arc of length ~80 Mpc in the Coma cluster, and regard fast encounters between nearby galaxies as the likeliest explanation of its properties.

Lavery & Henry (1988) first proposed that the Butcher–Oemler effect could be explained as star formation triggered by galaxy–galaxy interactions in intermediate-redshift clusters. A principal objection to this hypothesis was that the cluster velocity dispersion is typically too high (~1000 km s^{-1}) for strong tidal interactions to take place, since these require encounter speeds comparable to that of the galaxy rotation (Toomre & Toomre 1972). However, there has been increasing observational evidence for tidal effects on galaxies in both nearby and intermediate-redshift clusters, as well as theoretical work supporting the possibility of strong tidal fields in clusters. Numerical simulations have shown that within a few core radii of the centre of a rich cluster such as Coma, tidal compression of a galaxy by the cluster potential can produce spiral arms and tidal tails, and triggering of enhanced star formation (e.g. Byrd & Valtonen 1990; Valluri 1993; Henrikson & Byrd 1996). Moore et al. (1996) predict that fast close encounters with the central massive cluster galaxies will destroy many dwarf galaxies, and essentially transform spirals into ellipticals or dwarf spheroidals. All these simulations assume a fixed potential. However, the potential of a real cluster is expected to vary continually during its evolution with collapse of the cluster to virialization, and subsequent infall of additional material. Gnedin (1999) has used self-consistent cluster simulations to demonstrate that this time-varying potential will cause a sequence of strong tidal shocks on an individual galaxy, comparable to those from massive galaxies. The shocks, which are likely to be produced by surviving groups of galaxies or large individual galaxies, take place over a wide region of the cluster, and enhance galaxy–galaxy interactions as well as amplifying galaxy merger rates. A galaxy in a cluster similar to that of Abell richness class 0 or 1 at low redshift is predicted to have about four encounters closer than 10 kpc per Hubble time, and have a probability of about 30 per cent of being in a merger.

These results suggest that profound effects on cluster galaxy

morphology are to be expected from tidal forces during a Hubble time. In particular, Gnedin demonstrates that a likely consequence of tidal shocks is to turn a large fraction of normal spirals into S0s. This occurs by tidal heating of the disc, which reduces gravitational instabilities and suppresses further star formation. Gas is likely to be lost by ram-pressure stripping, interpenetrating encounters and, for low-mass galaxies, being blown out by starbursts. These results thus suggest that the same tidal forces which we have identified as causing circumnuclear starbursts in nearby clusters (and are evidently acting on cluster galaxies at intermediate redshifts) are the primary cause in transforming the spiral population in distant clusters into the S0 population in present-day clusters.

Any mechanism for converting spirals to S0s is required to be more efficient with increasing galaxy density for it to account qualitatively for the galaxy type–surface density (T–Σ) relation found for clusters at $z \sim 0.5$ and $z \sim 0$ (cf. Dressler et al. 1997). As has been seen in Section 4.3 above, the frequency of occurrence of tidally induced starbursts increases with increasing galaxy surface density, which implies that tidal forces do indeed act more efficiently on galaxies in higher density regions. This confirms that these forces are a suitable mechanism to account, at least qualitatively, for the T–Σ relation in clusters.

A further result, obtained in Section 4.3, is that the enhancement of tidally induced starbursts in cluster spirals is not wholly accounted for simply by an increase of local galaxy density. In addition, there is a 'cluster effect'. A spiral in a cluster of higher central galaxy density is more likely to undergo such a starburst than a spiral in a region of similar local density in a cluster with a lower central galaxy density. This implies that, in regions of comparable local density, the transformation of spirals into S0s proceeds faster in clusters of higher concentration and/or higher richness. This result suggests a simple explanation of the apparently anomalous absence of a T–Σ relation found by Dressler et al. (1997) for less concentrated, irregular clusters at intermediate redshifts.

Dressler (1980) had found a significant T–Σ relation for galaxies in both centrally concentrated 'regular' clusters and less concentrated, irregular clusters at $z \sim 0$, whereas by contrast Dressler et al. (1997) found a strong T–Σ relation only for regular clusters at $z \sim 0.5$. Unlike their counterparts at $z \sim 0$, irregular clusters at $z \sim 0.5$ have no significant T–Σ relation, and ellipticals in these clusters show no concentration to the densest regions. This is understandable if there has not been enough time for a significant transformation of disc galaxy morphology to take place in irregular clusters at $z \sim 0.5$. By contrast, such transformation would be expected for regular clusters at $z \sim 0.5$ (for which the time-scale for transformation is shorter) and for irregular clusters at $z \sim 0$ (for which a longer time duration for transformation is available). Furthermore, the same galaxy–galaxy and galaxy–group interactions responsible for the transformation of spirals to S0s may also cause ellipticals to relax to the densest regions in clusters over similar time-scales. Thus our finding of a 'cluster effect' in the enhancement of tidally induced starbursts and the consequent inference, for regions of similar local density, of an accelerated transformation of spirals to S0s in clusters of higher central density together provide a natural explanation for the apparently anomalous absence of a T–Σ relation for galaxies in irregular clusters at $z \sim 0.5$.

Finally, one may ask what mechanism may accelerate the rate of galaxy encounters (and consequent starburst activity), in clusters with greater central galaxy density? The work by Gnedin (1999) has shown that a time-varying cluster potential will enhance such encounters. Such a varying potential will arise both from cluster infall, and from subcluster mergers. Recent X-ray studies of a number of clusters have shown asymmetric X-ray morphologies and temperature structures which are consistent with those seen in simulations of subcluster mergers (e.g. Henriksen & Markevitch 1996; Honda et al. 1996; Donnelly et al. 1998; Henriksen, Wang & Ulmer 1999), implying that these clusters are recent post-merger systems. Furthermore, from a study of 10 distant clusters, Wang & Ulmer (1997) have shown that cluster global X-ray ellipticities correlate with their blue galaxy fractions. The strongly elongated clusters show substantial amounts of substructure, indicating that they are dynamically young systems, and leading Wang & Ulmer to suggest that the blue cluster galaxies originate in the process of cluster formation.

The above results thus suggest that subcluster mergers may be a mechanism to drive an accelerated rate of galaxy encounters and tidally induced starbursts (and consequent morphological evolution of disc galaxies) in more centrally concentrated clusters. One may suppose that such clusters have formed either as a result of subcluster mergers, or in higher density regions where the probability of such subcluster accretion is greater. The consequent accelerated rate of galaxy encounters and morphological evolution would account for a significant T–Σ relation for these clusters at $z \sim 0.5$, as compared to the absence of such a relation for the (presumably) relatively isolated irregular clusters at the same redshift.

According to this picture, a significant enhancement of starburst activity above that normally expected for galaxies in a region of a given density is expected in clusters which are still undergoing the effects of subcluster merger. By contrast, no such enhancement would be evident for clusters which are more relaxed. Such a scenario is entirely consistent with the results of our survey. The two most centrally concentrated clusters in the survey, Abell 1367 and Coma, both show evidence of being recent post-merger systems (Honda et al. 1996; Donnelly et al. 1998). Also, in accord with the expectation for such systems, spiral galaxies in these clusters have been found to have an enhanced starburst activity as compared to spirals in regions of similar density in less concentrated clusters.

6 CONCLUSIONS

From a survey of Hα emission in galaxies of types Sa and later in eight low-redshift Abell clusters, we have shown that circumnuclear starbursts, most probably triggered by tidal interactions (galaxy–galaxy, galaxy–group and galaxy–cluster), are more prevalent in spirals in denser regions and in clusters with a greater central galaxy density. In contrast to previous work, we find a monotonic increase in the fraction of spirals undergoing these starbursts from the field to higher density regions, and from clusters with low central galaxy density to clusters with high central density. There is a similar increase in the fraction of spirals classified as disturbed between the field and higher density environments, and between clusters of low and high central density. In the richest cluster studied (Coma), the fraction of spirals undergoing tidal distortion and/or tidally induced star formation appears comparable to the fraction of spirals showing these effects in rich clusters at $z \sim 0.5$.

From these results it is suggested that tidal interactions are the primary mechanism for an ongoing transformation of spirals to S0s in clusters, a scenario fully in accord with the most recent

models of clusters with a non-static potential undergoing collapse and infall. This mechanism can qualitatively account for the type–local surface density (T–Σ) relation found in clusters on account of the higher efficiency of the mechanism in higher density regions. Furthermore, the prevalance of tidally induced starbursts in spirals is found to depend not solely on local galaxy density, but also on cluster type. This implies that, for regions of comparable local density, transformation of spirals to S0s will take place faster in clusters with higher central density. This can account for the apparently anomalous lack of a T–Σ relation for irregular clusters at intermediate redshift. For these clusters there has not been time for significant morphological transformation of disc galaxies to have taken place, in contrast to regular clusters at intermediate redshift (for which the time-scale for transformation is shorter) and for low-redshift irregular clusters (for which a longer time interval is available during which transformations may take place). Moreover, it is suggested that subcluster merging is a cause of the enhanced starburst activity (and consequent accelerated morphological evolution of disc galaxies) seen in the denser clusters, as compared to regions of similar density in less dense clusters. The two richest clusters in our survey show evidence of being recent post-merger systems, whose galaxies have such enhanced starburst activity, consistent with this picture.

Finally, the fraction of late-type galaxies which are classified as peculiar (i.e., not in a recognizable stage of the Hubble sequence) also increases from the field to higher density environments, and from clusters of low to higher central density, in parallel with the increasing prevalance of tidally induced starbursts in spirals. A very high fraction (∼70 per cent) of these galaxies have emission similar to the starburst emission of spirals. It is suggested that these galaxies are predominantly ongoing mergers, which are expected as the end-product of some of the tidal interactions, and which are expected to be more common in regions of higher density and in clusters of higher central density due to the greater prevalence of tidal interactions in these locations.

ACKNOWLEDGMENTS

We thank the Institute of Astronomy, Cambridge, and CM thanks the Department of Astronomy, University of Virginia for hospitality in the course of this project. We also thank A. Biviano for helpful comments, and for kindly providing a Fortran code to estimate partial rank correlation coefficients using a bootstrap resampling technique. Observations were made with the Burrell Schmidt telescope of the Warner and Swasey Observatory, Case Western Reserve University. This research has made use of the NASA/IPAC Extragalactic Database (NED), which is operated by the Jet Propulsion Laboratory, California Institute of Technology, under contract with the National Aeronautics and Space Administration.

REFERENCES

Abell G. O., 1958, ApJS, 3, 211
Abell G. O., Corwin H. G., Olowin R. P., 1989, ApJS, 70, 1
Balogh M. L., Schade D., Morris S. L., Yee H. K. C., Carlberg R. G., Ellingson E., 1998, ApJ, 504, L75
Balzano V. A., 1983, ApJ, 268, 602
Baugh C. M., Cole S., Frenk C. S., 1996, MNRAS, 283, 1361
Bennett S. M., Moss C., 1998, A&AS, 132, 55
Biviano A., Katgert P., Mazure A., Moles M., den Hartog R., Perea J., Focardi P., 1997, A&A, 321, 84
Bushouse H. A., 1987, ApJ, 320, 49
Butcher H., Oemler A., 1978, ApJ, 219, 18
Byrd G., Valtonen M., 1990, ApJ, 350, 89
Conselice C. J., Gallagher J. S., 1999, AJ, 117, 75
Cowie L. L., Songaila A., 1977, Nat, 266, 501
de Jong R. S., 1995, PhD thesis, Univ. Groningen
de Vaucouleurs G., 1959, in Flügge S., ed., Handbuch der Physik, Vol. LIII. Springer-Verlag, Berlin, p. 275
de Vaucouleurs G., 1974, in Shakeshaft J. R., ed., Proc. IAU Symp. 58, The Formation and Dynamics of Galaxies. Reidel, p. 1
de Vaucouleurs G., de Vaucouleurs A., Corwin H. G., 1976, Second Reference Catalogue of Bright Galaxies. Univ. Texas Press, Austin (RC2)
de Vaucouleurs G., de Vaucouleurs A., Corwin H. G., Buta R. J., Paturel G., Fouqué P., 1991, Third Reference Catalogue of Bright Galaxies. Springer-Verlag, New York (RC3)
Donas J., Milliard B., Laget M., Buat V., 1990, A&A, 235, 60
Donnelly R. H., Markevitch M., Forman W., Jones C., David L. P., Churazov E., Gilfanov M., 1998, ApJ, 500, 138
Dressler A., 1980, ApJ, 236, 351
Dressler A., Oemler A., Butcher H. R., Gunn J. E., 1994, ApJ, 430, 107
Dressler A. et al., 1997, ApJ, 490, 577
Gavazzi G., Contursi A., 1994, AJ, 108, 24
Gavazzi G., Pierini D., Boselli A., 1996, A&A, 312, 397
Gavazzi G., Catinella B., Carrasco L., Boselli A., Contursi A., 1998, AJ, 115, 1745
Gnedin O. Y., 1999, PhD thesis, Princeton Univ.
Gunn J. E., Gott J. R., 1972, ApJ, 176, 1
Hameed S., Devereux N., 1999, AJ, 118, 730
Hashimoto Y., Oemler A., Lin H., Tucker D. L., 1998, ApJ, 499, 589
Heckman T. M., 1980, A&A, 87, 152
Henriksen M. J., Byrd G., 1996, ApJ, 459, 82
Henriksen M. J., Markevitch M. L., 1996, ApJ, 466, L79
Henriksen M. J., Wang Q. D., Ulmer M., 1999, MNRAS, 307, 67
Hernquist L., 1989, Nat, 340, 687
Ho L. C., Filippenko A. V., Sargent W. L. W., 1997a, ApJ, 487, 568
Ho L. C., Filippenko A. V., Sargent W. L. W., 1997b, ApJ, 487, 591
Honda H. et al., 1996, ApJ, 473, L71
Hubble E., Humason M. L., 1931, ApJ, 74, 43
Huchra J. P., Geller M. J., Clemens C. M., Tokarz S. P., Michel A., 1995, The CfA Redshift Catalogue, Version June 1995
Keel W. C., Kennicutt R. C., Hummel E., van der Hulst J. M., 1985, AJ, 90, 708
Kennicutt R. C., 1992, ApJ, 388, 310
Kennicutt R. C., 1998, ARA&A, 36, 189
Kennicutt R. C., Kent S. M., 1983, AJ, 88, 1094
Kennicutt R. C., Roettiger K. A., Keel W. C., van der Hulst J. M., Hummel E., 1987, AJ, 93, 1011
Koopmann R. A., Kenney J. D. P., 1998, ApJ, 497, L75
Lavery R. J., Henry J. P., 1988, ApJ, 330, 596
Mihos J. C., Hernquist L., 1996, ApJ, 464, 641
Miller R. H., 1988, Comm. Astrophys., 13, 1
Moore B., Katz N., Lake G., Dressler A., Oemler A., 1996, Nat, 379, 613
Moss C., Whittle M., 1993, ApJ, 407, L17 (Paper II)
Moss C., Whittle M., Irwin M. J., 1988, MNRAS, 232, 81 (Paper I)
Moss C., Whittle M., Pesce J. E., 1998, MNRAS, 300, 205(Paper III)
Nilson P., 1973, Uppsala General Catalogue of Galaxies. Uppsala Astron. Obs. Ann., 6 (UGC)
Noguchi M., 1988, A&A, 203, 259
Noguchi M., Ishibashi S., 1986, MNRAS, 219, 305
Oemler A., 1974, ApJ, 194, 1
Oemler A., Dressler A., Butcher H. R., 1997, ApJ, 474, 561
Paturel G., Bottinelli L., Gouguenheim L., 1994, A&A, 286, 768
Romanishin W., 1990, AJ, 100, 373
Sandage A., Tammann G. A., 1987, A Revised Shapley-Ames Catalog of Bright Galaxies. Carnegie Institution of Washington Publ. 635
Sanders D. B., Soifer B. T., Elias J. H., Madore B. F., Matthews K., Neugebauer G., Scoville N. Z., 1988, ApJ, 325, 74

Simien F., de Vaucouleurs G., 1986, ApJ, 302, 564
Smail I., Dressler A., Couch W. J., Ellis R. S., Oemler A., Butcher H., Sharples R. M., 1997, ApJS, 110, 213
Spitzer L., Baade W., 1951, ApJ, 113, 413
Strauss M. A., Huchra J. P., Davis M., Yahil A., Fisher K. B., Tonry J., 1992, ApJS, 83, 29
Struble M. F., Rood H. J., 1991, ApJS, 77, 363
Toomre A., Toomre J., 1972, ApJ, 178, 623
Trentham N., Mobasher B., 1998, MNRAS, 293, 53
Valluri M., 1993, ApJ, 408, 57
Valluri M., Jog C. J., 1990, ApJ, 357, 367
van den Bergh S., 1976, ApJ, 206, 883
van den Bergh S., 1997, AJ, 113, 2054
Wallenquist A., 1960, Medd. Uppsala Astron. Obs., No. 127
Wang Q. D., Ulmer M. P., 1997, MNRAS, 292, 920
Wright G. S., Joseph R. D., Robertson N. A., James P. A., Meikle W. P. S., 1988, MNRAS, 233, 1
Zwicky F., Herzog E., Wild P., Karpowicz M., Kowal C., 1960–1968, Catalogue of Galaxies and Clusters of Galaxies, Vols. 1–6. California Inst. Tech., Pasadena (CGCG)

This paper has been typeset from a TEX/LATEX file prepared by the author.